REPORT DOCUMENTATION PAGE

Form Approved
OMB NO. 0704-0188

1. AGENCY USE ONLY (Leave Blank)	2. REPORT DATE	3. REPORT TYPE AND DATES COVERED
	Aug 23, 2006	Final Report May 1, 2001 – July 30, 2006

4. TITLE AND SUBTITLE
Design Rules for High Temperature Microchemical Systems

5. FUNDING NUMBERS
DAAD 19-01-1-0582

6. AUTHOR(S)
Rich Masel

7. PERFORMING ORGANIZATION NAME(S) AND ADDRESS(ES)
University Of Illinois, Urbana Champaign

8. PERFORMING ORGANIZATION REPORT NUMBER

9. SPONSORING / MONITORING AGENCY NAME(S) AND ADDRESS(ES)
U. S. Army Research Office
P.O. Box 12211
Research Triangle Park, NC 27709-2211

10. SPONSORING / MONITORING AGENCY REPORT NUMBER

11. SUPPLEMENTARY NOTES
The views, opinions and/or findings contained in this report are those of the author(s) and should not be construed as an official Department of the Army position, policy or decision, unless so designated by other documentation.

12 a. DISTRIBUTION / AVAILABILITY STATEMENT
Approved for public release; distribution unlimited.

12 b. DISTRIBUTION CODE

13. ABSTRACT (Maximum 200 words)

The key objective of the work so far was to do the science needed to design better microburners and microreactors for soldier power and other applications. Microcombustion has gone from "impossible" to routine. Microreactors for ammonia reforming shrank by more than a factor of 100. Computational models exist where none existed before.

14. SUBJECT TERMS
Microreactor, Microburner, Soldier Power

15. NUMBER OF PAGES
34

16. PRICE CODE

17. SECURITY CLASSIFICATION OR REPORT	18. SECURITY CLASSIFICATION ON THIS PAGE	19. SECURITY CLASSIFICATION OF ABSTRACT	20. LIMITATION OF ABSTRACT
UNCLASSIFIED	**UNCLASSIFIED**	**UNCLASSIFIED**	**UL**

NSN 7540-01-280-5500

Standard Form 298 (Rev.2-89)
Prescribed by ANSI Std. 239-18
298-102

Final Report

Design Rules for High Temperature Microchemical Systems

Richard I. Masel, PI
Department of Chemical Engineering
University Of Illinois
Box C-3 Roger Adams Lab
600 S Mathews Avenue
Urbana IL, 61801
(217)333-6841 (Phone), (217)333-5052 (fax)
e-mail: r-masel@uiuc.edu

Administrative Point of Contact:
Charles Zukoski,
Research Board,
1901 S First St Suite A,
Champaign Il 61820-7406
voice: (217) 333-2187, fax: (217) 333-2189

Agreement Number: DAAD 19-01-1-0582

Contract Period: May 1, 2001 – July 30, 2006

Report Date: Oct 25, 2006

1. RESEARCH OBJECTIVES:

The overall objective of the proposed research is:

To develop the science base, fabrication technologies, transport laws, and design methodologies in order that a wide range of high temperature microchemical systems may be developed. In particular, we are interested in developing design guidelines for microburners and design guidelines to combine microburners and microreactors to produce integrated units.

To reach this objective, we have formulated a program composed of four individual tasks: 1. Design rules for microburners (experiments: Masel, Shannon, Short; simulations: Short, Vlachos) 2. Monolithic microreactors for the production of hydrogen (experiments: Masel, Seebauer; simulations: Vlachos) 3. Fabrication and testing of ceramic and metallic microreactors (Kenis) 4. Thermal management and thermal integration (Shannon, Masel)

2. EXECUTIVE SUMMARY

The key objective of the work so far was to do the science needed to design better devices for soldier power and other applications. Table 1 shows a perspective on the results. Microcombustion has gone from "impossible" to routine. Microreactors for ammonia reforming shrank by more than a factor of 100. Computational models exist where none existed before.

Table 1 A perspective on the UIUC accomplishments

	Status at project beginning	Status at project end
Microcombustion	Most investigators question whether microcombustion is possible	Microcombustion routine Flame structure, dynamics characterized
Microreactors	20 W ammonia reformer ***300 cm^3*** No propane micro reformers	20 W ammonia reformer ***1 cm^3*** Propane steam reforming without coking, catalyst deactivation
Models	No computational models of	Computational models exist

2.1 Microburners

One of the key accomplishments of the UIUC effort was to demonstrate stable microburners for the first time. Prior to Masel and Shannon's work microcombustion was thought to be impossible. In 2000 Masel and Shannon demonstrated that microcombustion was possible, but the burners only lasted for 8 hours, due to the very high temperatures in the flames. One key accomplishment in the UIUC MURI effort was to create stable high temperature microburners. The approach took advantage of the fact that flow on the microscale is laminar not turbulent, so that one can run parallel fuel and air streams, and have them only slowly mix by diffusion. The effect is that one can spread the flame over a wide area instead of creating a hot spot that melts the walls. This technique was demonstrated experimentally, and we created microburners that were stable for months.

Another accomplishment was to observe the structure of microflames for the first time and to compare them to conventional flames and available calculations. It was found that microscale flames are not anything like flames on a larger scale. Isolated flame balls and other discontinuous structures are seen rather than continuous lifted flames. The structures are stable over a wide range of stoichiometric conditions and exist for both methane and propane. These results show that combustion on the microscale is fundamentally different than combustion on a larger scale.

The UIUC team also did computations of the flame structure. Generally the calculations gave reasonable predictions of the stability limits of the flames, but the detailed flame structure was not accurately predicted. Instead, only continuous flames were seen in the computations.

Visualization was used to try to determine why the flames were the shapes we observe. Generally, when the burners are cool no stable flame structures are observed. Instead there is a transient phenomenon, where flames ignite, and travel down the centerline of the burner, and are then extinguished. As the walls heat, flame cells are slowly stabilized. Detailed examination of the structures indicates that the flames are hook flames.

Hook flames are well understood theoretically. They arise because of a transition between premixed and laminar diffusion behavior. This suggests that the mechanism of flame cell formation is as given in Figure 6. We start with a standard laminar diffusion flame which quenches due to heat transfer to the walls. Once the flame quenches, diffusion can occur, mixing the fuel. The fuel reignites leading to premixed hook flames.

At this point the UIUC group believes that they have a good qualitative picture why the flame structures exist. There is, however, still a significant difference between computation and experiment.

2.2 Microreactors

A second main goal in the MURI program is to create design guidelines for robust microreactors for the production of hydrogen. The approach is to start with a simple fuel, ***ammonia***, work out how to build microreactors, and then move up to a more complex fuel, propane. Ammonia was chosen for our initial work because the fuel is of some interest to the Army, the reaction kinetics are simple, and there is only one reaction pathway: $2\ NH_3 \rightarrow N_2 + 3\ H_2$. Also, the equilibrium conversion increases as the reactor temperature increases. Barton from MIT has shown that there is considerable advantage in running ammonia decomposition in a high temperature microreactor.

The UIUC team pioneered the use of monolithic anodized aluminum as an alternative catalyst support. Reactors created in the acceptable surface area-to-volume ratios while withstanding considerable shaking, avoiding bypassing of reactants, and promoting temperature uniformity due to structural continuity. Over the years the UIUC group made significant improvements to the design. The reaction rate was raised by a factor of 50. The pressure drop in the beds was reduced. At the end of the project we were able to produce microreactors with a surface areas and catalytic activity comparable to pack beds, but with a pressure drop that is a small fraction of that in a packed bed.

Another key finding is that changes in reactor geometry make a tremendous difference in performance. Channel reactors generally show plug flow behavior while posted reactors show considerable mixing. Flow visualization using smoke to image the flow shows that the channel reactor behaves like a PFR, while the posted reactor shows considerable mixing. Importantly, there are considerable fluctuations in the flow with the posted reactor. Pulse testing of the reactors also suggests large fluctuations in the flow in the posted reactor.

Calculations were done to understand these results. Generally, the calculations show that transient flow fluctuations cause there to be much more mixing in the posted reactor than in the channel reactor.

The UIUC team has also developed reactors for the production of hydrogen from propane using SiCN and SiC monolithic inverted opal catalyst monoliths (impregnated with Ru catalyst) into their alumina reactor housings to obtain an all-ceramic microreactor. These microreactors

have a unique combination of properties: low pressure drops due to high porosity of the monoliths (0.73), high surface areas of 10^7 m^2/m^3, and thermal stability up to 1200°C.

2.3 Thermal management

The UIUC team had a seed effort in thermal management. One key part of the effort finding conditions for stable conditions in microreactors and microburners, where heat generation was sufficient to maintain a stable temperature, but there was not so much heat produced that walls melted. Models gave criteria, but there was never a good agreement between models and experiment. One key unexplained experimental observation was that once stable flame balls formed, they were very difficult to extinguish by for example cooling the walls.

Another seed effort was to try to identify some new materials that were highly reflective and still were stable in a high temperature oxidizing environment. We tested a number of oxides, particularly titanium dioxide, tantalum pentoxide since a number of previous investigators have used these oxides as low temperature radiation shields. Much of the effort was devoted to developing fabrication procedures for the materials as thick films of the oxides have not yet been reported in the literature. Also, we needed to develop techniques to measure the reflectivity at high temperature.

2.4 Quantitative measures

So far the workers supported by this project have presented 86 talks on work supported by the MURI, and 55 articles were prepared for journal submission. A total of 25 students and postdocs were partially supported by the contract. So far the UIUC MURI program has lead to two DARPA programs that translate aspects of the work into practice: R. I. Masel, PI "MicroGC with Nanotube, Nanogate and Microm8 Detectors" and R. I. Masel, PI, "Porous silicon fuel cell systems for micro power generation" A third DARPA program is pending.

2.5 Recommendations for future work

Considerable progress has been made in the MURI effort. We now have stable microburners and microreactors with acceptable pressure drops. Three areas, though, need further work: i) materials for thermal management ii) modeling of the reactors and burners, and iii) reactor design guidelines. Materials for thermal management is a key need. During the MURI work, the UIUC group tested a number of materials as insulators and heat spreaders, and none were totally satisfactory. Available were either too fragile for use, or required an insulating thickness that was larger than the devices that are being. Radiation shields were a problem. Many materials stay reflective if they are connected to an external UHV vacuum pump, but quickly lose reflectivity under the normal conditions. Heat spreaders were also a problem. One would like switchable heat spreaders that are insulating when the system is warming up, but become conducting when the operating temperature is reached. The UIUC group never found suitable switchable heat spreading materials. Thus, a new effort on materials for thermal management is needed.

Another key need is for better models for the microreactors and microburners. At present there is still a substantial gap between experiment and computation for microreactor and microburner design. Closing that gap would be another key thrust for future work.

A third need is design guidelines for microreactors. The UIUC group has produced working microreactors optimized for particular reactions: ammonia reforming and propane reforming If one wanted a reactor for another purpose, one would need to do extensive experiments One would like to have design guidelines that allowed one to design a reactor without needing extensive experimentation.

Table 2 Summary of the key accomplishments of the MURI

New Science	New Devices
■ Flame structure in microcombustion ■ Hook Flames ■ Models ■ Design equations for microreactors ■ Flow visualization ■ RTD ■ Computational Techniques ■ Unsteady 3D models	■ Low pressure drop microreactors ■ Reliable microburners ■ Tailored high temperature, high surface area materials, catalysts ■ Active catalysts ■ Integrated reactor/combustor ■ New thermal isolation structures

3. HIGHLIGHTS:

Tables 1 and 2 summarize our key findings. More details are in the sections below.

3.1 Microburners

One of the key accomplishments of the UIUC effort was to develop stable microburners. To put this work in perspective, Jensen, Masel, Moore and Shannon demonstrated microcombustion for the first time, but these devices only lasted 8 hours, and many investigators thought that Jensen at al were observing heterogeneous not homogeneous combustion. Consequently new designs were needed.

We changed to alumina burners like those in Figure 4. These are simple machined alumina structures that had been treated using a procedure developed under the UIUC MURI so that the surfaces are inert. These were the first devices to show stable microcombustion without failure.

Another key accomplishment of the UIUC effort was to measure the structure of microflames for the first time and to compare them to conventional flames and available calculations. Previously the UIUC team found that microscale flames are not anything like flames on a larger scale. Isolated flame balls and other discontinuous structures are seen rather than continuous lifted flames, as seen in Figure 1 and Figure 2. The structures are stable over a wide range of stoichiometric conditions and exist for both propane and oxygen. These results show that combustion on the microscale is fundamentally different than combustion on a larger scale.

In our previous grant period the UIUC team also did computations of the flame structure. Generally the calculations gave reasonable predictions of the stability limits of the flames, but the detailed flame structure was not accurately predicted. Instead, only continuous flames were seen in the computations.

Work in the last year concentrating on closing the gap between theory and experiment. One part of the work was to use flow visualization to see if any fluid instabilities, flame stretch, or other effects were causing the differences between theory and experiment. One experiment was to inject smoke in the inlet and search for vortex sheading or other fluid instabilities. Figure 3 shows some of these results. Notice that the smoke travels along a straight path as it moves through the burner. Therefore it appears that the fluid instabilities are not causing the instabilities.

The effects of flame stretch were also examined, but no significant effects were seen.

Next visualization was used to try to determine why the flames were the shapes we observe. Figure 4 and Figure 5 show some of the structures that have been observed. Generally, when the burners are cool we observe smooth laminar diffusion flames such as those shown in Figure 4. Such flames are not stable unless there is an external heat source, such as a flame at the exit of the burner. As the burner heats, flame cells such as those in Figure 5, are seen. These flame structures are stable when the external heating is removed. Detailed examination of Figure 5 shows that the structures are hook flames.

Figure 1 Picture of the burner during operation. Notice: the flame has split into three distinct flame balls.

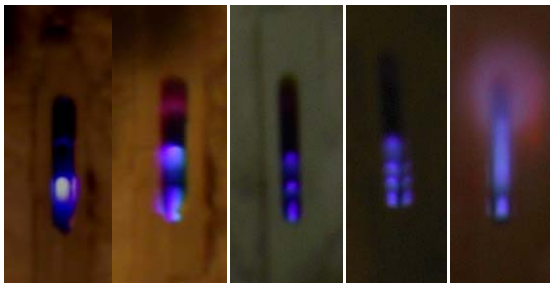

Figure 2 Some of the flame structures that have been observed in the experiments.

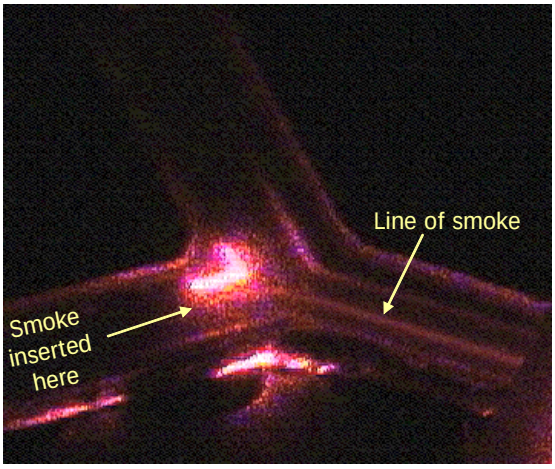

Figure 3 Flow visualization showing the flow pattern in the burner. Notice that the flow is steady and laminar

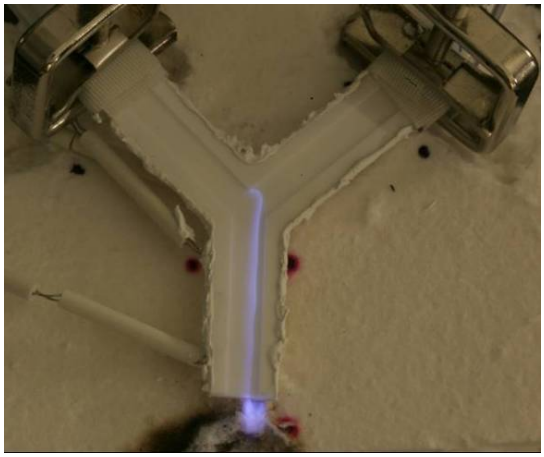

Figure 4 Pictures of a cool burner with a continuous looking flame. This flame is not stable. Instead the flame at the exit of the burner ignites the flame and the flame quickly quenches.

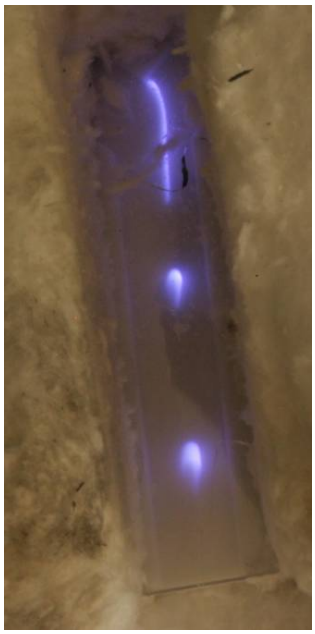

Figure 5 Hook flames seen when the burner was heated and the external heat source extinguished.

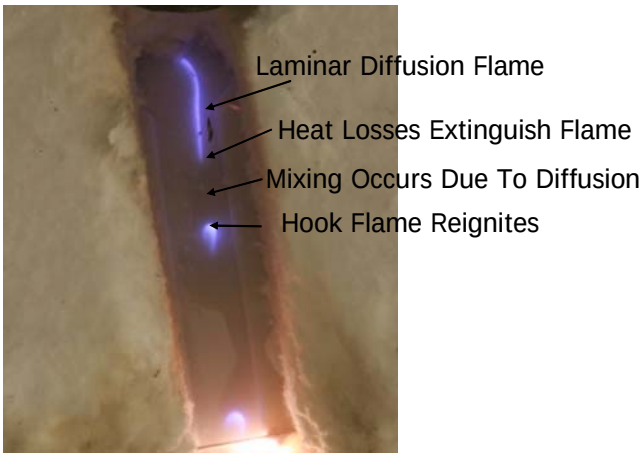

Figure 6 The mechanism of formation of the flame cells

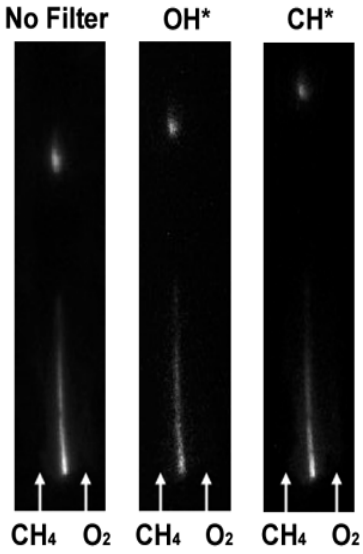

Figure 7 Slowly evolving flames seen when the external heat source extinguished with different optical filters.

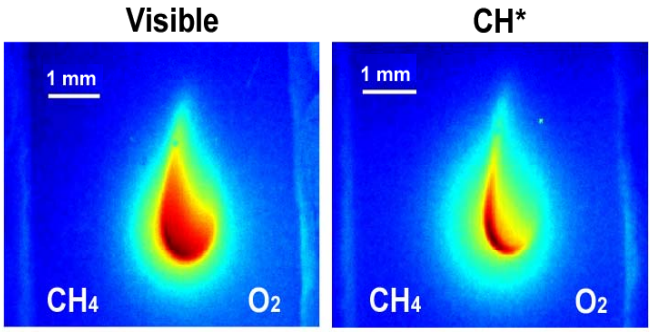

Figure 8 Closeup false-color photographs of the flame cells chemiluminescence intensities in the visible light range and for the CH* radical emission band.

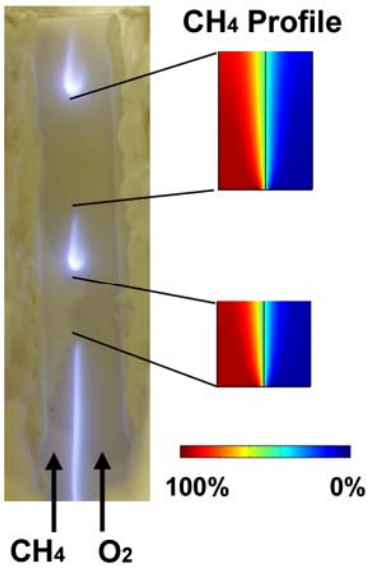

Figure 9 Slowly evolving flames seen when the external heat source extinguished with different optical filters.

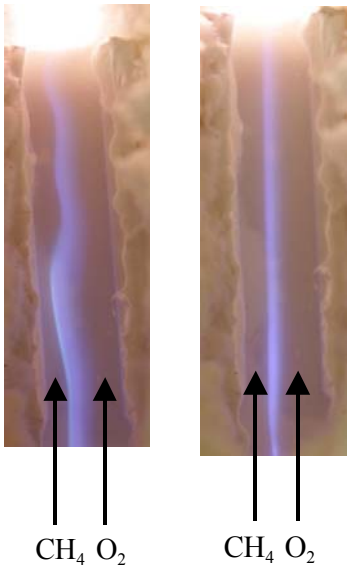

Figure 10 Ignition of a flame involves a complicated sequence of events, which are only slightly apparent in these still photographs of the flame just a few seconds after ignition of the cone flame.

Steady state hook flames are well understood theoretically. They arise because of a transition between premixed and laminar diffusion behavior. This suggests that the mechanism of flame cell formation is as given in Figure 6. We start with a standard laminar diffusion flame which quenches due to heat transfer to the walls. Once the flame quenches, diffusion can occur between the laminar streams, mixing the fuel and oxygen. In the region of the flames, there is

significant emission of the dominate hydroxyl and methyl radicals, as shown in Figure 7 . Closeup false-color photographs of the chemiluminescence intensities in the visible light range and for the CH* radical emission band shown in Figure 8 show that flames are most intense in the premixed region at the bottom of the flame cell and nearest the fuel rich side. The methyl radicals quench rapidly away from the highest intensity part of the flame. From our earlier work [Prakash *et al.*, 2005] we demonstrated that OH* radicals have very low chemical action on alumina surfaces prepared the way we developed for these burners. Hence, once the fuel is consumed within the flame region, the flame extinguishes. Diffusional mixing occurs, as illustrated in Figure 9, supplying a premixed *and* preheated fuel/oxidizer source for the next flame structure. The flame cells are stabilized at the position by the flame speed equaling the flow speed of the reactants, which are the same velocity. The flame speed is determined predominately by the temperature of the reactants, and secondarily by the wall temperature. Supply high degrees of cooling to the walls shifts the flame cell location only slightly. As the walls heat up and cool, the flame cells evolve slowly to a new axial position. It is important to note that the flame cells are only present when anchored laminar diffusion flame exists. At the anchor point, the flow velocity of the impinging flows is near zero, since it is a stagnation point. Hence, the flame speed needed to stabilize the flame against the flow is near zero. Hence the temperature of the incoming reacting gases does not need to be high as in the channel itself. This is a key observation for creating stable flame cells at specific locations.

The dynamic process leading to the steady-state flame has also been studied and now is also qualitatively understood. The ignition of a flame involves a complicated sequence of events, which are only slightly apparent in these still photographs of the flame just a few seconds after ignition of the cone flame. As shown in Figure 10, the flame appears to wiggle laterally in the channel and then straighten out. However, this is not a steady process. As seen in Figure 11, high-speed photography shows that on ignition there is a series of traveling flames that come down from the cone flame and then anchor at the base where the fuel and oxidizer come together. This cycle occurs periodically for several minutes of time, as the walls heat up and the flame cells begin to stabilize, as seen in Figure 12. This process produces audible sound, with distinct regimes, as shown in a time trace in Figure 13 of a microphone signal that records the emitted sounds. These regimes correspond to the wall temperatures, as shown in Figure 14.

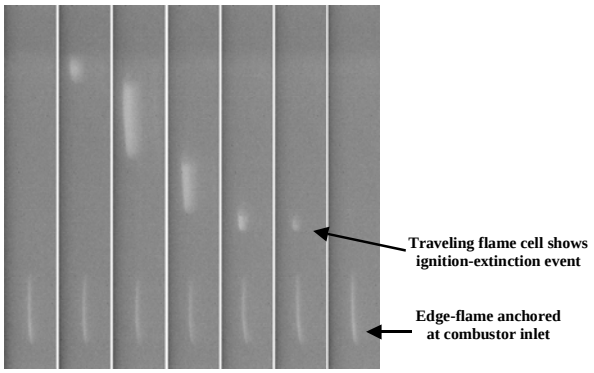

Figure 11 High-speed photography of ignition of flame. Flame initially starts from cone flame on top and travels to anchor point. Flames repeatably follow at specific frequencies.

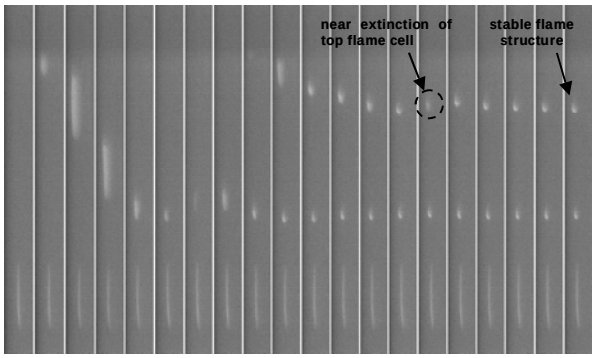

Figure 12 The mechanism of formation of stable flame cells

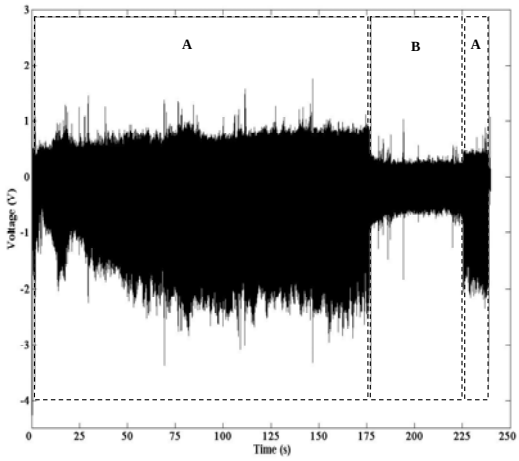

Figure 13 An acoustic emission signal as a function of time after ignition. There are three distinct regimes of sound, corresponding to the type of flame dynamics. At stabilization there are no sounds emitted

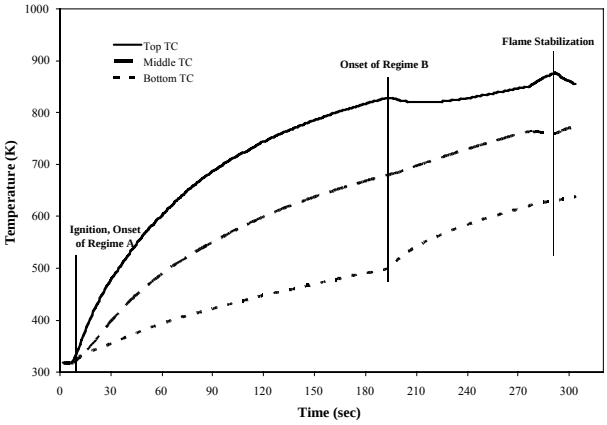

Figure 14 The temperature evolution of the walls corresponding with the different flame dynamic regimes. At flame onset in regime A, there are low-frequency sounds. In regime B there are loud, whistle like and high frequency sounds. Wall temperatures determine the regime.

Examining the frequency domain of the emitted sound shown in Figure 15, we note that the initial low frequencies correspond to the extinction-ignition events seen in Figure 11 and Figure 12. There are also high-frequency components that correspond to flame-structure interactions with the burner, the various modes of which can be seen in Figure 16. The main conclusion that we can draw from this data is that on startup, the flame within the burner moves from the hotter to cooler section of the burner, and the gases within the burner have strong spatial and temporal variations in temperature, giving rise to a wide variety of flame-fluid-structure interactions. As the walls heat up and the flame gas temperatures stabilize and reach a critical point, the dynamics cease and the flame structures vary slowly with wall temperature.

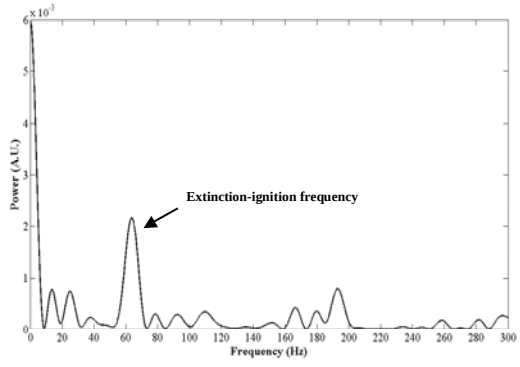

Figure 15 An acoustic emission signal as a function of time after ignition. There are three distinct regimes of sound, corresponding to the type of flame dynamics. At stabilization there are no sounds emitted

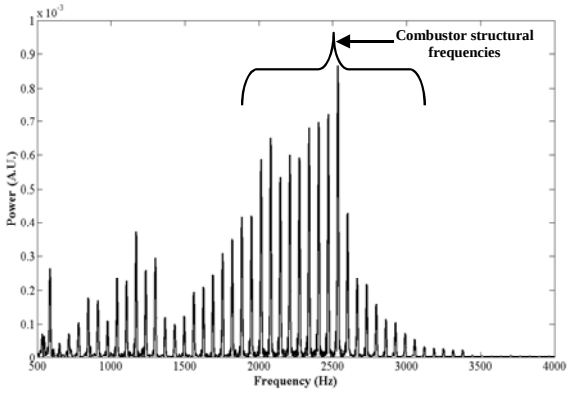

Figure 16 The temperature evolution of the walls corresponding with the different flame dynamic regimes. At flame onset in regime A, there are low-frequency sounds. In regime B there are loud, whistle like and high frequency sounds. Wall temperatures determine the regime.

At this point the UIUC group believes that they have a good qualitative picture why the flame structures exist. There is, however, still a significant difference between computation and experiment that needs to be resolved. To resolve this difference, on going simulations are carried out that indicate that diffusion flames, studied experimentally, could differ from premixed flames that have been modeled so far. These simulations start closing the experiment-theory gap.

Another key part of the effort was to develop models for the microcombustion. Vlachos is using a 46 reaction set to model methane-air. His group studies the propagation of methane flames through micron size tubes. Work in other geometries, which represent our experimental efforts, is under way. Most simulations have been based on the parabolic flow approximation that has minimal computational cost. However, in order to address the thermal management, elliptic simulations will also be conducted.

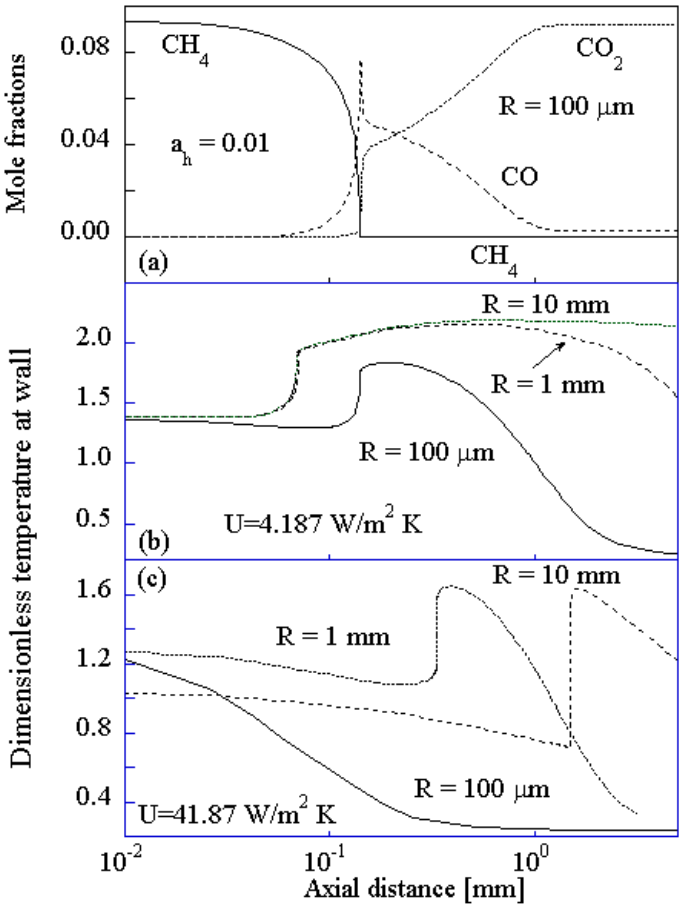

Figure 17 Concentration and temperature profiles during methane combustion in a round tube for various values of the tube diameter and wall heat transfer coefficient.

Figure 17 shows the results of some calculations for premixed methane air for various values of the wall heat transfer coefficient and flame tube diameter. Notice that the flame propagates in a 10 mm tube under all of the conditions studied. However, flame propagation is less likely in a 100 μm tube. According to the calculations a methane air flame does not

propagate through the tube unless the heat transfer coefficient to the surroundings is less than $1x10^{-4}$ cal/(cm^2 K sec), i.e. the burner needs to be very well insulated. Qualitative results in burners with millimeter gaps, the thermal discontinuity at the walls controls quenching. With 100 micron gaps, the loss of radicals dominates. Some key routes to loss of radicals at the walls are: $2H \rightarrow H_2$, $CH_3 + H \rightarrow CH_4$, $2CH_3 \rightarrow C_2H_6$.

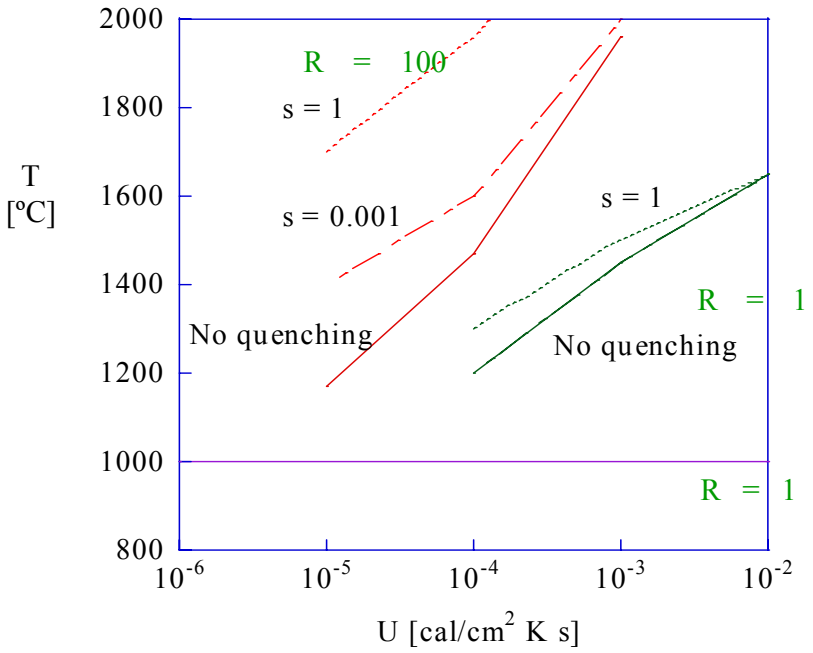

Figure 18 The temperature needed to get flames to propagate through round tubes as a function of the wall heat transfer coefficient and the sticking probability of radicals on the walls of the tube for three tube radii.

Figure 18 shows the temperature needed to get flames to propagate through round tubes as a function of the wall heat transfer coefficient and the sticking probability of radicals on the walls of the tube. Notice that a sticking probability as small as 0.001 can reduce the reaction rate enough to quench the flame in microreactors. This is a very different feature from large scale chemical reactors (e.g., the 1 cm radius reactor).

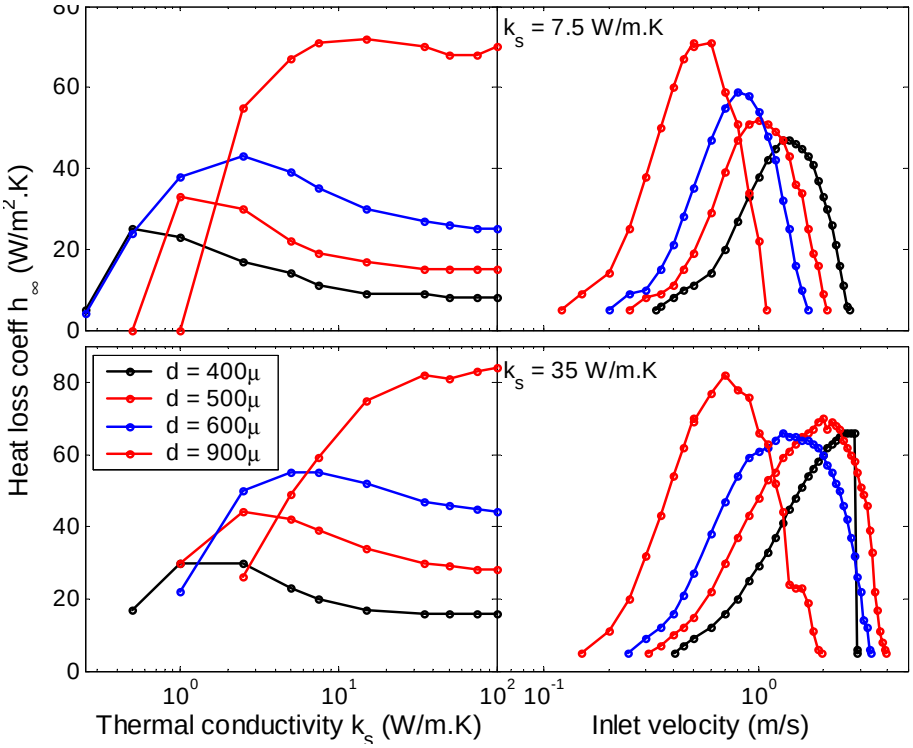

Figure 19 Effect of reactor gap width on quenching characteristics of propane/air mixtures. Larger channels can sustain combustion at higher heat losses. Increased recirculation results in an extension of the blowout limit for smaller channels.

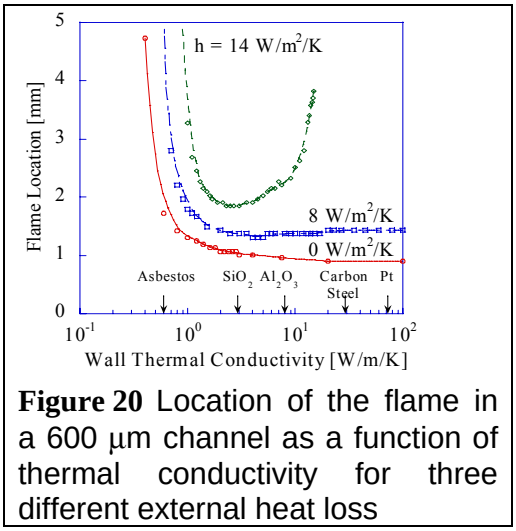

Figure 20 Location of the flame in a 600 µm channel as a function of thermal conductivity for three different external heat loss

Large scale simulations were also done to try to model the behavior of the UIUC burners. In the first year, the primary effort was to determine how radical and thermal quenching determines the fundamental extinction limits of the methane-air system. The model utilized the boundary layer approximation for cylindrical microchannels and incorporated detailed gas-phase chemistry (46 reactions) as well as radical quenching reaction mechanisms. The primary finding from that work is that radical and thermal quenching become significant below a critical diameter. As the sticking coefficient of radicals on walls increases, lower external heat losses or higher inlet temperatures are required for flame propagation. It was shown that in a tube with a radius of 1 cm, flames propagate under all conditions. The time scale for heat and mass transport to the wall from the center of the tube is long enough that the flame cannot be extinguished, regardless of the external heat losses or sticking coefficient. However, flame propagation in 100 µm radius tubes is much less likely. Even a sticking coefficient of 10^{-3} has a significant effect on flame stability.

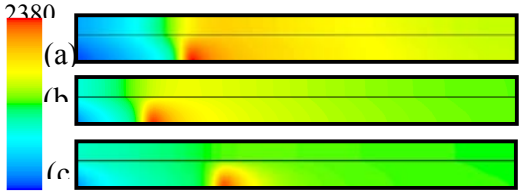

Figure 21 Temperature contours [K] for h=14 W/m^2/K with wall thermal conductivity of k_w=1.1 (a), 3.0 (b) and 14.0 W/m/K (c). The parameters are channel gap L=600 μm, wall thickness L_w=200 μm, flow velocity V = 0.5 m/s.

In the second year, the role of heat transfer within the system was considered in detail. A fully elliptic model is used that accounts for 2D heat and mass transport within the fluid and 2D heat transport within the walls. This elliptic model allows self-sustained flames with room temperature feeds to be modeled (a desirable situation mode). As Masel and Shannon have improved the process to make the reactor material "quenchless", the focus of this work has shifted from stopping radical quenching to thermal management that improves flame stability and minimizes hot spot generation. To achieve this goal an irreversible, one-step chemistry has been used. Work focused initially on methane and has recently been extended to propane.

The materials of construction of the reactor play a vital role in the overall thermal management of the system. The thermal conductivity of the wall is orders of magnitude greater than that of the fluid. Consequently, much of the upstream heat transfer that preheats the cold incoming feed, occurs within the walls. Figure 20 shows the location of the flame in the channel as a function of wall thermal conductivity for three different external convective heat loss coefficients. Figure 21 shows temperature contours within the reactor for three different wall thermal conductivities.

The main conclusions from these simulations can be outlined as follows:

1. For a given heat loss or heat exchange, there is an optimum wall thermal conductivity (see Figure 20 and Figure 21). When the wall thermal conductivity is too low, the upstream heat transfer through the walls is limited and blowout occurs. When the wall thermal conductivity is very high, the wall temperature becomes nearly isothermal. This increases the available hot wall area for external heat losses causing thermal quenching. This optimum wall conductivity allows for maximum heat loss or exchange without loss of stability (see Figure 23) and appears to be in the range of high temperature ceramics, such as alumina and silica.
2. There is an optimum flow velocity that results in enhanced flame stability.
3. There is an optimum gap distance. Figure 22 shows contours of temperature for different gap sizes. For large gap sizes (>1 mm), the flame is shifted downstream. Flames are very stable, hot spots form, and the ignition distances are too long (blowout may occur). Medium gap sizes (~1 mm) exhibit lower maximum wall temperatures and earlier flame locations. Small gap sizes (400 μm) have greatly reduced fluid and wall temperatures. The reaction zone in these cases is delocalized and the flame stability is low.
4. Small gap microburners are susceptible to oscillations. When there are heat losses and the system is close to extinction, operation in microburners becomes unstable, leading to periodic oscillatory behavior. The location of the reaction zone/flame location shifts quickly as a function of time. Large temperature swings within the fluid are shown with an amplitude >1400 K. The heat recycle from the hot walls causes a temperature rise much above the adiabatic flame temperature. However, the wall temperature and exit temperature remain nearly constant. High frequency (~1 kHz) pressure variations of > 100 Pa in this example are observed. These pressure variations may be equally critical to burner stability.
5. Qualitatively, propane behaves similarly to methane. However, propane appears to have a larger range of conditions that allow for stabilized flames. Larger exterior heat transfer is

allowed for a given wall thermal conductivity, and smaller minimum wall thermal conductivities are feasible than methane (see Figure 23). Methane flames are sustainable within the range of free convection (2-25 W/m^2/K for gases), whereas the propane flames are stable even in the low end of the forced convection (25 – 250 W/m^2/K for gases). Furthermore, flame temperatures vary more drastically with conditions and are lower than those of methane microburners. Finally, higher flow velocities are possible without extinguishing or blowing out the flame. The observed behavior indicates greater microburner stability for propane/air mixtures.

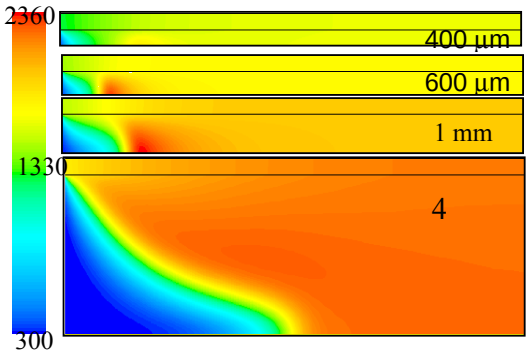

Figure 22 Contours of temperature [K] for different gap separations, L. Wider channels must be long to preheat enough for ignition (blowout is possible). Smaller channels give lower temperatures but are more susceptible to extinction.

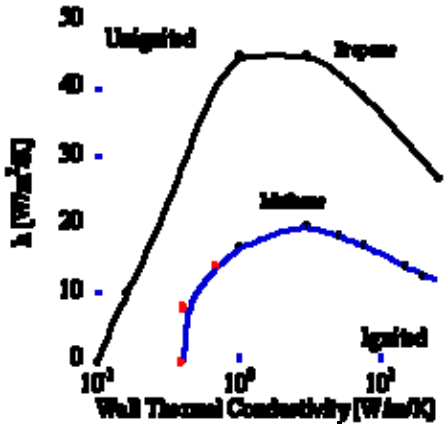

Figure 23 Stability diagram for methane and propane combustion in a microburner. The plotted points indicate blowout or extinction and the line is a smooth interpolation of the points. The parameters are V=0.5 m/s, L=600 µm, and L_w=200 µm.

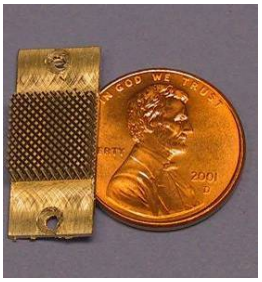

Figure 24 A posted reactor for the production of hydrogen from ammonia.

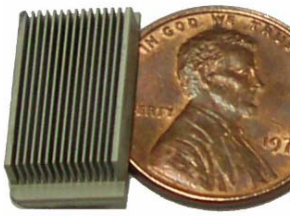

Figure 25 An improved reactor for the production of hydrogen from ammonia

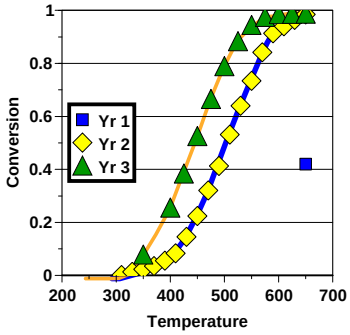

Figure 26 The conversion of 145 sccm of ammonia in the various reactors built under this MURI.

3.2 Microreactors

A second main goal in the MURI program is to create design guidelines for robust microreactors for the production of hydrogen. The approach is to start with a simple fuel, ***ammonia***, work out how to build microreactors, and then move up to a more complex fuel,

propane. Ammonia was chosen for our initial work because the fuel is of some interest to the Army, the reaction kinetics are simple, and there is only one reaction pathway: $2\ NH_3 \rightarrow N_2 + 3\ H_2$. Also, the equilibrium conversion increases as the reactor temperature increases. Barton from MIT has shown that there is considerable advantage in running ammonia decomposition in a high temperature microreactor.

In the first year, the UIUC team pioneered the use of monolithic anodized aluminum as an alternative catalyst support. Recall that beds of conventional catalyst particles are often not sufficient durable to be used in a portable microchemical device. Bypassing is a significant problem as is loss of catalyst.

The objective of this part of our work is to develop robust catalyst designs. In particular we have explored production of microreactors using micro electro discharge machining (μEDM) and anodization and by electrodeposition. We have also done a heat balance on these reactors so we had design data for design of the burners.

One part of the work is to explore μEDM and anodization as a way of producing robust reactor structures for the microscale. Recall that μEDM has previously been used to produce micron scale flow channels, but the extension to micro reactors is not obvious. One needs to find ways to add catalyst and to insure that the resultant structure is sufficiently robust to survive.

The addition of the catalyst represents a key issue for the production of robust structures. Catalysts can be added to ceramic microstructures using sol-gel techniques, but sol-gel coatings on metal substrates are known to not be robust upon thermal cycling. Silica coatings work if only oxides are used as a catalyst, but metals such as platinum sinter rapidly on silica substrates. We were interested in using transition metal catalysts. Consequently, we decided to try something else.

Our approach is to use anodization to produce a porous layer over an aluminum substrate. Previously, anodized foils have been used as catalysts. There has been some speculation that other anodized structures could be used in microreactors. However, details were lacking.

We have done several experiments to determine what types of anodized microreactor structures could work, and to characterize the reactor performance for the production of hydrogen from ammonia.

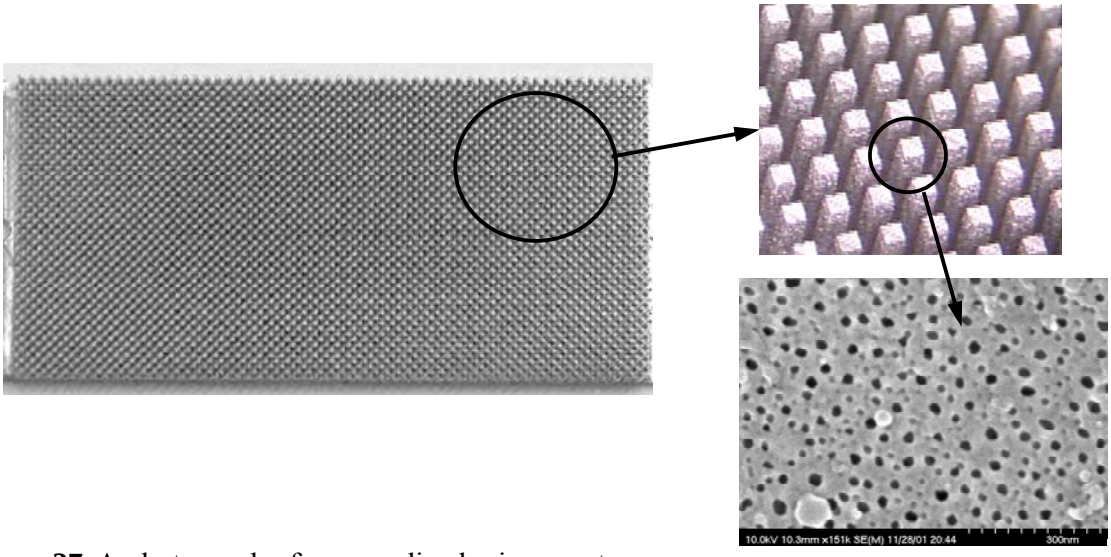

Figure 27 A photograph of our anodized microreactor.

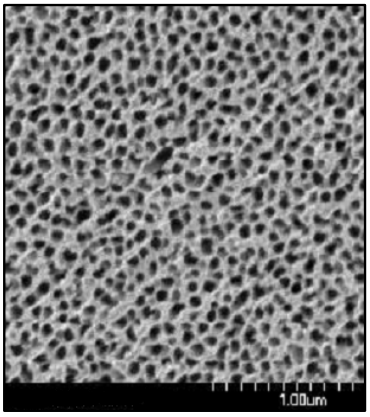

Figure 28 SEM of an anodized aluminum post (1100 aluminum)

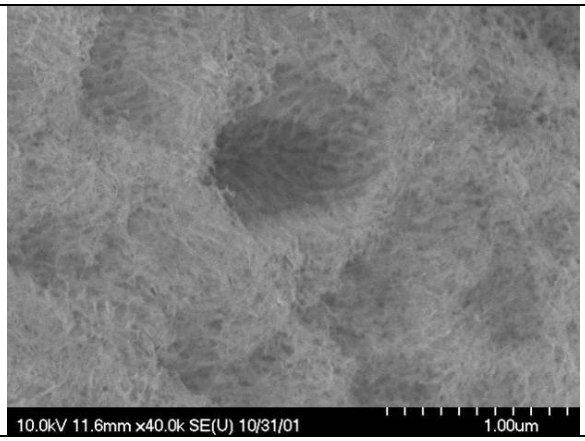

Figure 29 SEM of an anodized alumina post (6061 Aluminum)

Figure 27 shows a photograph of our first microreactor. This reactor is 1 inch wide aluminum covered by 500 micron wide, 3 mm high diamond posts on 1000 micron centers in a diamond pattern. The surface of each post has been anodized to produce a 36 micron layer of alumina in which platinum has been deposited. The post also shrink during anodization. 500 micron posts shrink to 300 microns.

Figure 28 and Figure 29 compare the anodization of different aluminum alloys. We find when metallurgical pure aluminum is anodized, the reactor gives a high surface area material. On the other hand, anodized 6061 aluminum does not have as high of a surface area. BET analysis shows that anodized 1100 aluminum has a surface area 1000 times higher than it physical area, while anodized 6061 aluminum has a surface are that is too small to measure using the available techniques.

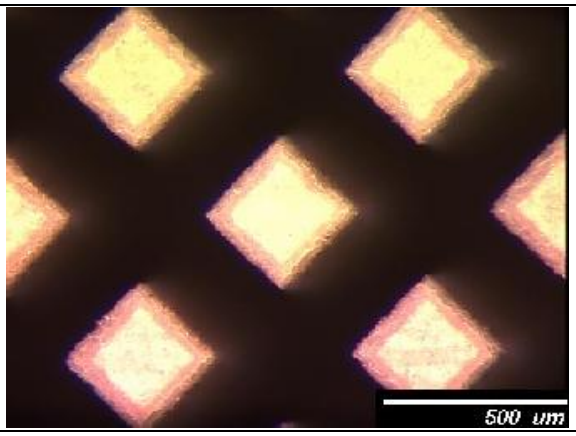

Figure 30 An optical photograph of a 1100 aluminum reactor that has been anodized at 30 V.

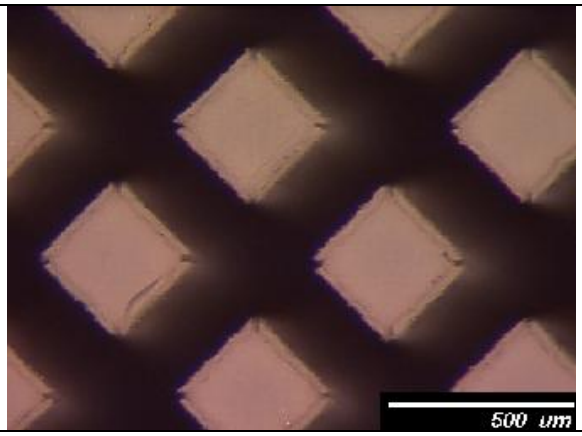

Figure 31 An optical photograph of a 1100 aluminum reactor that has been anodized at 60 V.

We have also varied our anodization conditions. Figure 30 and Figure 31 show the results. We find that if anodize at 30 V, we get a 50 micron thick layer that adheres upon thermal cycling. On the other hand if we anodize at 60 V, we end up with a layer that cracks and flakes off upon thermal cycling.

Reactors such as that shown in Figure 24 and Figure 25 can support acceptable surface area-to-volume ratios while withstanding considerable shaking, avoiding bypassing of reactants, and promoting temperature uniformity due to structural continuity. The first three years were devoted to improving the design. Figure 26 shows how the performance changed over the first three years of the grant. We were able to substantially improve the performance of the reactor.

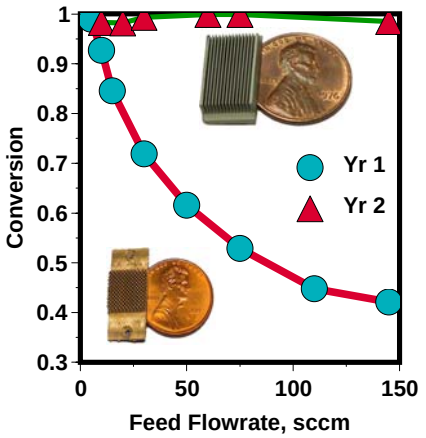

Figure 32 A comparison of the performance of the reactors in Figure 24 and Figure 25.

Work in the last two years concentrated on trying to understand the differences in performance we see in Figure 32 where channel reactors show much higher conversion than posted reactors. Simulations done in year 3 did not indicate that there was a large difference between the two reactors. Yet experimentally, the performance was quite different. The object of the work in year 4 was to close the gap between theory and experiment.

The experiments included measuring kinetics of the reaction, comparing performance to idealized behavior, flow visualization, RTD measurement and mapping to approximate equations. Figure 33 and Figure 34 show some of kinetic measurements started in yr 3 and completed in yr 4. Experimentally, the conversion in the posted reactor is as expected for a CSTR, while the conversion in the channel reactor is as expected for a PFR. Flow visualization using smoke to image the flow shows that the channel reactor behaves like a PFR, while the posted reactor shows considerable mixing. Importantly, there are considerable fluctuations in the flow with the posted reactor. Pulse testing of the reactors shown in Figure 37 also suggests large fluctuations in the flow in the posted reactor. This suggests that one of the main causes of the difference between calculation and experiment, was that the calculations assumed steady flow, while the experiments show mixed flow. Figure 38 shows the results of calculations needed to verify this idea. Generally, the calculations show that transient flow fluctuations cause there to be much more mixing in the posted reactor than in the channel reactor. At this point there is still a difference between theory and experiment, since the calculations were done in 2D to save computer time, while the experiments are 3D. However, the reason for the remaining difference between theory and experiment have been identified and suitable calculations are in progress.

The theoretical development has also lead to an important result: one can characterize the mixing in our devices in terms of an effective diffusivity. Recall that according to the standard Taylor-Aris analysis all reactors should show CSTR behavior in the limit of rapid diffusion of all of the reactants and products. Vlachos and coworkers have shown that one can define an effective diffusivity for a reactor, to account for the extra mixing in a posted reactor. Computations show that the effective diffusivity for the posted reactor is much higher than that in the channel reactor, which partially accounts for the difference in behavior. At this point there is still a difference between theory and experiment, since the calculations are 2D, while the experiments are 3D. 2D calculations take about a week of computational to converge. 3D

calculations have not yet converged. Still, the path to eliminate the remaining difference between theory and experiment is clear. Modeling has provided design guidelines in terms of post density, catalyst loading, and post shape.

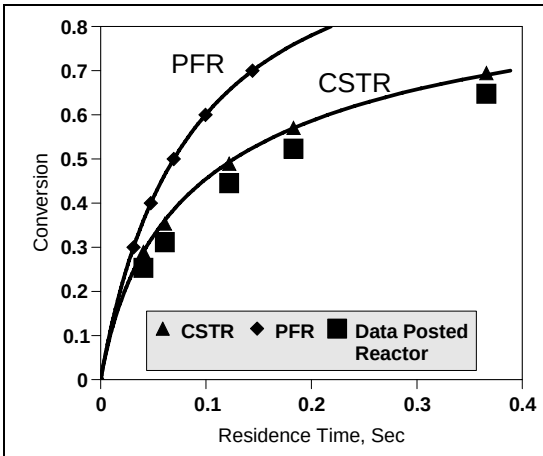

Figure 33 A comparison of the performance of the posted reactor in Figure 24 to that for an ideal PFR and CSTR.

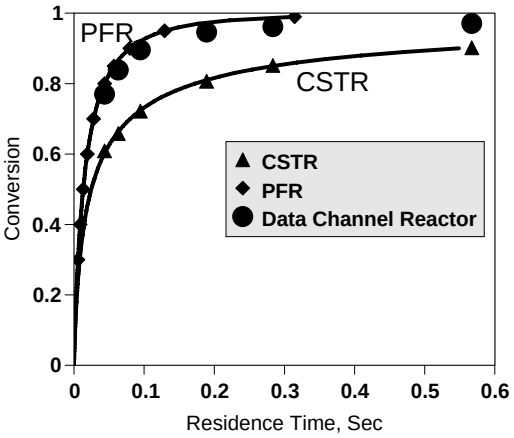

Figure 34 A comparison of the performance of the channel reactor in Figure 25 to that for an ideal PFR and CSTR.

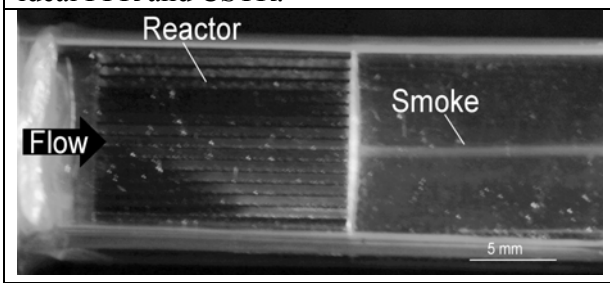

Figure 35 A picture of the flow pattern in the channel reactor. Smoke inserted in the beginning of the reactor emerges as a smoke line at the end of the reactor.

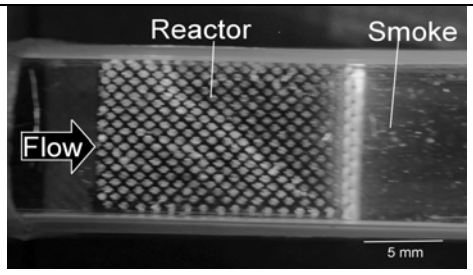

Figure 36 A picture of the flow pattern in the posted reactor. Smoke inserted in the beginning of the reactor emerges as a well mixed cloud at the end of the reactor.

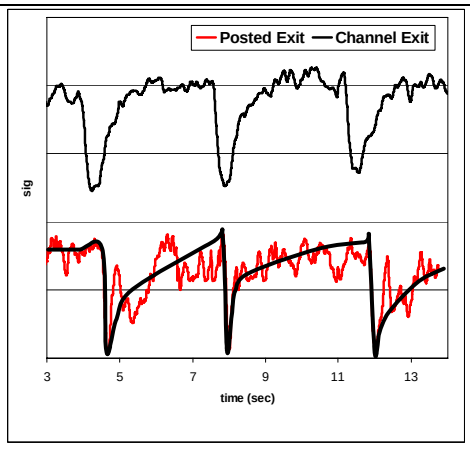

Figure 37 Pulse testing of the reactors

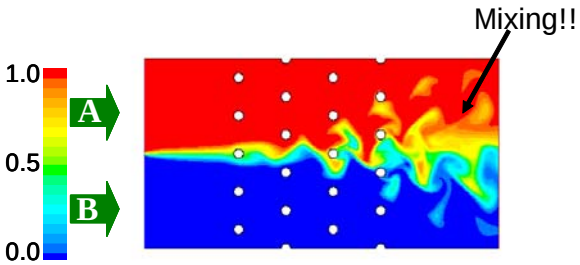

Figure 38 2D unsteady calculation of the flow in a posted reactor

The UIUC team has also started working on **microreactors for the production of hydrogen from propane**. Kenis and coworkers have integrated their highly porous SiCN and SiC catalyst monoliths (impregnated with Ru catalyst) into their alumina reactor housings to obtain an all-ceramic microreactor (Figure 39). These microreactors have a unique combination of properties: low pressure drops due to high porosity of the monoliths (0.73), high surface areas of 10^7 m^2/m^3, and thermal stability up to 1200°C (Adv. Funct. Mat., 2004). Characterization of A Ru loading of 4.5 wt.% was determined for these SiC monoliths after impregnation with Ru catalysts, while the dispersion of active metal phase was ~20 % (J. Catalysis, 2005).

Ammonia decomposition: Using a tube furnace as the heat source, the decomposition of ammonia into hydrogen and nitrogen was studied as a function of temperature (450 – 1000°C) for different entering ammonia flow rates (Figure 40). Complete conversion of NH_3 was reached between 750 and 950 ºC for flow rates between 3 and 36 sccm of NH_3. At 36 sccm of NH_3, a maximum of 54 sccm of H_2 was produced from a reactor with a monolith volume of only 0.55 mm^3. So, 10^5 sccm H_2 is produced per cm^3 of monolith volume, which is two orders of magnitude more than the highest number reported in literature. Comparing turnover frequencies provided a key explanation for this excellent result: The Ru/SiC structures (this work) exhibit about 10 times higher catalytic activity compared to Ru/SiO_2 or Ru/Al_2O_3 (literature). The microreactor structures do not show signs of failure after >15 thermal cycles of >8 hours each at temperatures as high as 1000 ºC. Also, no catalyst deactivation is observed after exposing the reactor to 12 sccm NH_3 at 800 ºC & 1000 ºC for 48 h each (J. Catalysis, 2005).

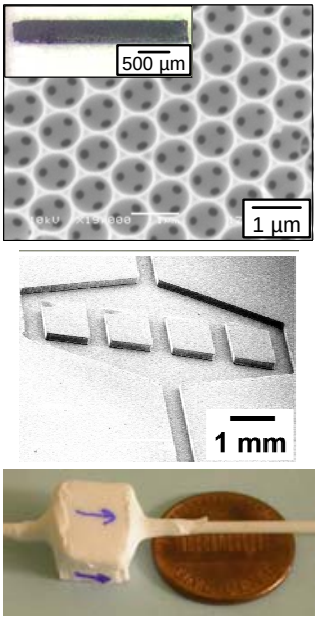

Figure 39 (left) Top: SEM of inverted-opal SiC catalytic monolith structure, here with 0.75 micron pores (inset: whole structure). Middle: Alumina reactor housing. Bottom: Assembled ceramic microreactor comprising five Ru/SiC catalyst support structures, integrated into the ceramic housing.

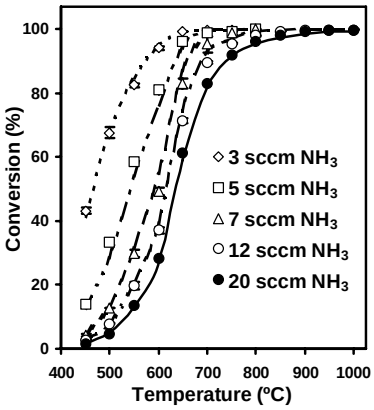

Figure 40 (right) Ammonia decomposition for different flowrates as a function of temperature in a ceramic microreactor.

Propane steam reforming: We also tested these microreactors for steam reforming of propane. One of the main problems faced in reforming of hydrocarbons is coking of the catalyst structures, resulting in catalyst deactivation. Coking issues can only be avoided if the reaction is performed at temperatures above 800 °C. Our microreactors comprised of Ru/SiC monoliths mounted in alumina housings can sustain such temperatures as shown already for ammonia decomposition. We thus tested our reactors for propane steam reforming, again using a tube furnace as the heat source, and we varied steam-to-carbon ratios, temperature, flow rates, and monolith pore size. In all reactors, full conversion of propane could be obtained, resulting in a mixture of predominantly hydrogen and CO, with only trace amounts of CO_2 and other partial

decomposition products (Figure 41). As always, the CO formed in steam reforming needs to be led through a water gas shift reactor to obtain an additional 25% of hydrogen, while also recovering some of the heat in this exothermic reaction. Full conversion of propane could be reached at temperatures as low as 850°C, while maintaining a steam-to-carbon ratio of 1.1. Note that the lower the S/C ratio, the less energy is needed to heat the steam to the operation temperature of the reactor. We obtained a maximum of 22 sccm H_2 which corresponds to 10^4 sccm H_2/cm^3 monolith, while using a certain amount of helium as the carrier gas to allow for quantification. Without the helium, even higher production of hydrogen is to be expected. The hydrogen selectivity was typically on the order of 75-80%. Even after thousands of hours of operation at 800-1000°C, no coking of the reactor and no catalyst deactivation was observed as shown in Figure 42, showing the high mechanical and thermal stability of these microreactors under operating conditions. The propane conversion and hydrogen selectivity data were identical within 0.3% with the values obtained before thermal cycling.

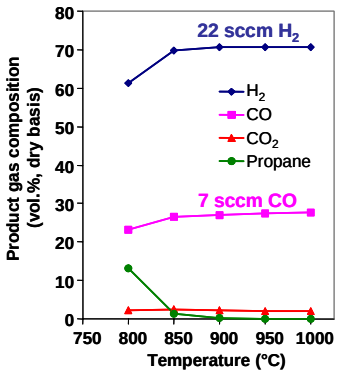

Figure 41 (left) Typical product gas composition as a function of temperature for propane steam reforming in a Ru/SiC ceramic microreactor.

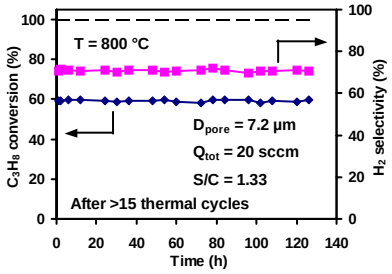

Figure 42 (right) Stability test: No change in conversion and hydrogen selectivity over time, even after >15 cycles at 800-1000 °C.

Reactor scaling: We also created microreactors with a higher fraction of their overall volume being SiC monoliths, moving from 5 to 18 monolith pieces per reactor. As expected, higher absolute conversion of propane into hydrogen was obtained.

Novel washcotas for propane reforming: The UIUC team has also begun creating catalyst washcoats for propane reforming. Propane reforming catalysts usually have limited lifetime at high temperatures due to catalyst sintering. Titania has been found to reduce sintering, but the anatase phase of titania is not stable at high temperature, so titania additions have not proven to work in practice. Masel and coworkers now have developed a new procedure to keep the titania stable.

3.3 Thermal Management

The UIUC team has also continued a low level effort on thermal management. We have also done simulations to understand how thermal coupling affects reactor performance. Thermal coupling between the two reactors is crucial, as illustrated in Figure 43.

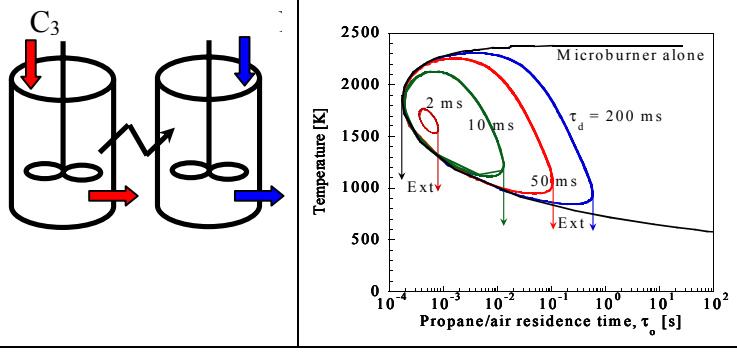

Figure 43 Schematic of coupled CSTR reactors. The plot shows the temperature as a function of the propane combustion residence time for various NH_3 decomposition residence times.

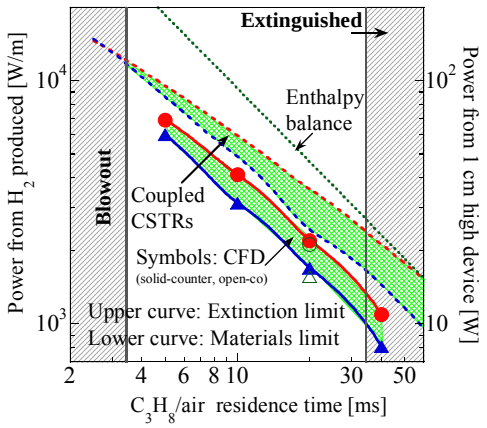

Figure 44 Operation map indicating the power generation from coupled devices, using a hierarchy of models ranging from CFD to simple reactors.

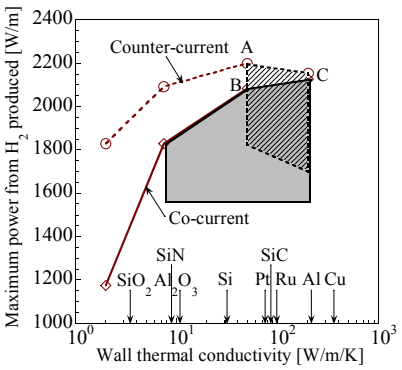

Figure 45 Maximum power generated based on the hydrogen produced as a function of wall thermal conductivity for the two configurations. The propane/air inlet flow velocity is 0.5 m/s. The shaded region demarcates the operation windows delimited by extinction and materials stability (see text). The counter-current operation is slightly better in a narrow window (region ABC). The co-current configuration allows a wider choice of fabrication materials and catalysts. The points represent the simulation data and the lines only guide the eye.

CFD calculations were also carried out with propane combustion and ammonia decompostion in adjacent reacting channels. Two flow configurations, viz. co-current and

counter-current, have been compared in terms of various performance criteria including device temperatures, maximum power exchanged, temperature of exit gas stream, and hydrogen production achieved. Best configurations have been identified. Finally, operation maps have been created to enable one to do proper balancing of flow rates for various flow rates of H_2, as shown in Figure 44.

The effect of flow configuration, namely co- vs. counter-current flow, on the operation of multifunctional microdevices for hydrogen production has been analyzed using two-dimensional computational fluid dynamics simulations. Stoichiometric propane/air gaseous combustion and ammonia reforming on Ru occur in alternate parallel channels separated by a thermally conducting wall. The power generated is in the range of 8-60 W per cm height of the device depending on flow rates. A proper balance of the flow rates of the combustion and reforming streams is, however, crucial in achieving this. For either configuration, the maximum power generated is determined by extinction at large reforming stream flow rates. Materials stability, resulting from high temperatures generated at low reforming stream flow rates, determines the lower power limit for a given flow rate of combustible mixture, as shown in Figure 44. The two flow configurations are found to be practically equivalent for highly conductive materials (see Figure 44). Using properly balanced flow rates, the co-current configuration expands the operation window to medium as well as low thermal conductivity materials as compared to the counter-current configuration that shows a slightly superior performance but in a rather narrow regime of high ammonia flow rates and high thermal conductivity materials.

The UIUC group has explored the use of thin-film based reflective radiation shields for thermal management. Whenever homogenous combustion occurs in millimeter or sub-millimeter scales, the wall and flame temperatures tend to be very high (the wall temperatures are ~1000°C). High wall temperatures make vacuum packaged heat shields difficult to construct and the shields must be able to endure oxidizing conditions. Hence dielectric materials like tantalum pentoxide (Ta_2O_5) that have good high temperature structural properties, resistance to oxidation and low optical absorption in the IR are better candidates for the construction of reflective thin film radiation shields. An immediate problem that arises is the lack of thermal radiative optical constants in the IR for such dielectric materials. Data at the relevant high temperatures of operation was found to be absent in current literature for dielectric materials including Ta_2O_5. The IR optical constants at both room and high temperatures are being calculated using IR reflectance measurements using an FTIR equipped with a reflectometer. The room temperature FTIR setup has been used to calculate the optical properties of as-deposited Ta_2O_5. In addition, as a first step in understanding the high temperature optical properties of dielectric materials, the effect of prior exposure to high temperature on the room temperature radiative optical constants of thin films of Ta_2O_5 deposited on Si and SiO_2 was studied. The IR optical constants of both crystalline Ta_2O_5 and the material interface formed between the Ta_2O_5 and the Si substrate were calculated and presented in literature for the first time (Figure 21).

High temperature reflectance measurements are currently being pursued. As it turns out, significant issues arise in measuring optical properties at high temperature in FTIR's, due to the effect of emission on the system. We therefore developed a new methodology for making these measurements, and have tested the method with gold and Si films, which are among the few matierals where the index of refraction, *n,* and the extinction, *k,* coefficients are known at high temperatures. A publication describing this method is being prepared. Preliminary reflectance data has also been collected using this method for a variety of materials including Si and Ta_2O_5. The absorptance for many materials increase with temperature, making their use in IR reflectors

problematic. The initial reflectance measurements show that the optical properties of Ta_2O_5 do not change significantly when heated to temperatures as high as 500°C (Figure 22), which is important for the oxide reflectors to operate as desired. The high temperature reflectance should be in publishable form within the next report.

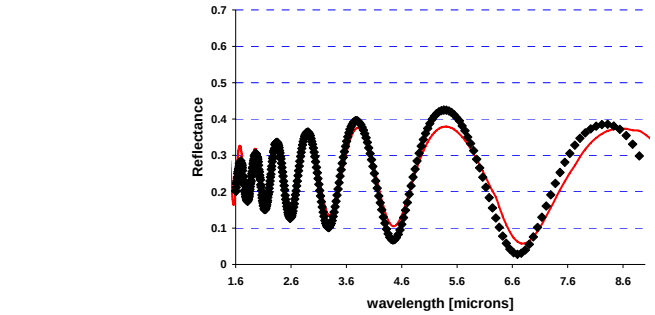

(a)

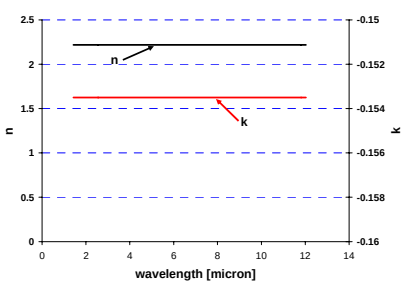

(b)

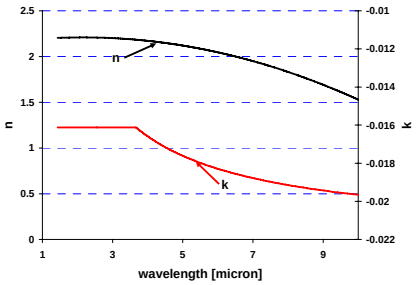

(c)

Figure 46 *a) Comparison of the measured (dotted) and predicted (complete line) reflectance for crystalline Ta_2O_5 heated to 900°C for 9 hours. b) n and k values as a function of wavelength for the interfacial layer between film and substrate c) n and k values for the Ta_2O_5 film.*

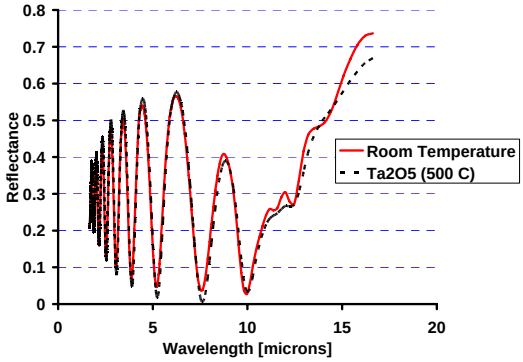

Figure 47 *Comparison of the measured (dotted) and predicted (complete line) reflectance for crystalline Ta_2O_5 heated to 900°C for 9 hours.*

The UIUC group has also started to examine a new class of insulating structures that use quantum effects, i.e. band gaps to limit the flow of heat. Figure 49 shows some photonic band structure calculations we have done to verify the idea. If we are able to build the structure in Figure 48, it should completely block radiant heat transfer at wavelengths between 2 and 6 microns, and have partial reflections at other frequencies. Conduction should also be unusually low because of the staggered post structure.

In summary then, at this point, the UIUC group has made significant progress on the initial goals of the MURI. They have developed design rules for microburners and microreactors. These design rules have allowed better systems to be built. There is still more work to be done, but significant progress has occurred.

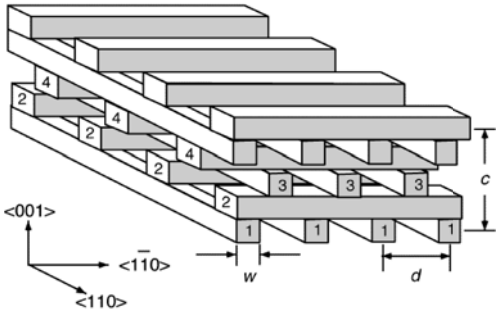

Figure 48 Insulator formations that are expected to have very low transmission of heat due to gaps in the phonon transmission bands.

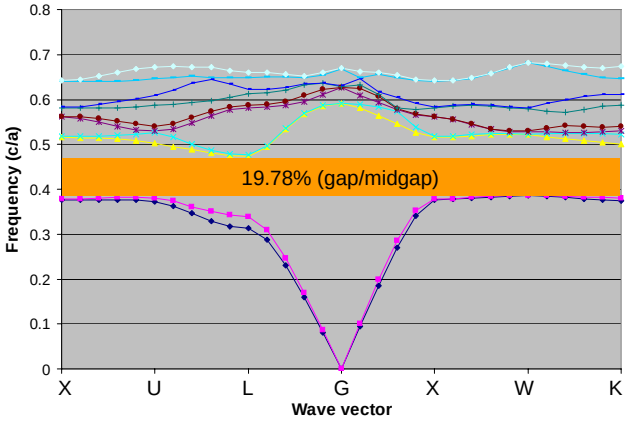

Figure 49 Photonic band structure calculated for the formation in Figure 48.

4. SUPPLEMENTARY MATERIAL:

The following faculty were partially supported by the project:

Faculty	Individual contribution
Richard Masel (PI)	Burner measurements, Reactor measurements, Catalyst development
Mark Shannon	LIF Measurements, Thermal isolation, Collaborate on burner measurements
Dionisios Vlachos	Burner stability calculations, Reactor design equations
Paul Kenis	High T compatible reactor structures, Propane steam reforming, catalyst monolith and microreactor characterization
Edmund Seebauer	Collaborate on reactor measurements, Collaborate on catalyst development
Mark Short	Flame ball calculations, Collaborate on flame ball measurements

The following junior personnel were partially supported by the grant:

Student	Expected Degree	Advisor
Jason Ganley	PhD, ChE (2004)	Masel and Seebauer
Craig Miesse	PhD, ChE (2005)	Masel and Short
Michael Mitchell	PhD, ChE (2006)	Kenis
Inkyu Park	MS, MIE (2003)	Shannon
Shaurya Prakash	MS/PhD, MIE in progress	Shannon with Masel
Ramesh Chandrasekharan	PhD, MIE, in progress	Shannon with Masel
Daniel Norton	MS/PhD, ChE	Vlachos
Stephanie Raimondeau	PhD, ChE (2003)	Vlachos
Soumitra Deshmukh	MS/PhD, ChE	Vlachos
Nicholas Ndiege	PhD, Chem in progress	Masel with Shannon
Kate Riechmann	BS, ChE (2006)	Masel
Christian	PhD, ChE (2006)	Kenis
David Dempsey	BS, ChE (2003)	Kenis
Bobby Feller	BS, ChE (2003)	Kenis
Marina Lebedeva	Postdoc, ChE	Vlachos
James Hammonds	PhD, MIE (2003)	Shannon
Robert Larson	ChE, PhD in progress	Masel
Ashish Mhadeshwar	PhD, ChE	Vlachos
Richard Zheng	PhD, Chem expected 2006	Masel with Seebauer
Adarsh Radadia	PhD, ChE, in progress	Masel
J. Dalton York	MS, ChE (2004)	Masel
Ian Sung	Visiting Scholar (student)	Kenis
Ravi Subramanan	Visiting Scholar (postdoc)	Masel and Seebauer
Dr. Don Kim	Visiting Scholar (Faculty)	Kenis
Hae-Kwon Joeng	Visiting Scholar (postdoc)	Masel and Shannon
A. D. Armijos	Ms, MIE (2006)	Shannon
Niket Kaisare	Postdoc, ChE	Vlachos

5. TALKS/PRESENTATIONS/PUBLICATIONS:

5.1 Presentations

1) R.I. Masel (speaker), P.J.A. Kenis, M.A. Shannon, E. Seebauer, D. Vlachos, *High Temperature Microchemical Systems*, Palm Power Meeting, Arlington VA, Sept 2001
2) D.G. Vlachos, *Recent advances in multiscale modeling of oxidation microreactors*Department of Mechanical and Aerospace Engineering, Univ. of Southern California, Los Angeles CA, Feb. 13, 2002
3) R.I. Masel (speaker), P.J.A. Kenis, M.A. Shannon, E.G. Seebauer, D.G. Vlachos, *High Temperature Microchemical Systems*, Palm Power Meeting, Panama City FL, Mar 2002
4) R.I. Masel, *Microburners, Micro fuel converters and Micro Fuel Cells*, Department of Chemical Engineering, U. I. Chicago, Chicago IL, Apr 2002
5) R.I. Masel (speaker), P.J.A. Kenis, M.A. Shannon, E.G. Seebauer, D.G. Vlachos, *Progress In High Temperature Microchemical Systems*, Palm Power Meeting, Panama City Fl, March 2002

6) R.I. Masel (speaker), P.J.A. Kenis, M.A. Shannon, E.G. Seebauer, D.G. Vlachos, *Progress In High Temperature Microchemical Systems*, Palm Power Meeting, San Diego Ca, Feb 2003
7) D. G. Vlachos, "Microchemical Systems for Lightweight Multifunctional Structures", ARL, Aberdeen, MD, April 17, 2003.
8) D. G. Vlachos, "From chemistry to design concepts of portable fuel processing devices", Catalysis Center, Northwestern University, Oct. 29, 2003.
9) D. G. Vlachos, "From chemistry to design concepts of portable fuel processing devices", Department of Chemical Engineering, Lehigh University, Nov. 12, 2003.
10) A. B. Mhadeshwar, H. Wang, and D. G. Vlachos, "Thermodynamic Consistency in Microkinetic Development of Surface Reaction Mechanisms", 226 ACS Fall Meeting, New York, NY Sept. 7-11, 2003.
11) D. G. Norton and D. G. Vlachos, "The Role of Fuel in the Stability of Exothermic Microchemical Systems", 226 ACS Fall Meeting, New York, NY Sept. 7-11, 2003.
12) S. R. Deshmukh, A. B. Mhadeshwar and D. G. Vlachos, "Microkinetic Modeling of Ammonia Synthesis & Decomposition on Ruthenium and Microreactor Design for Hydrogen Production", 226 ACS Fall Meeting, New York, NY Sept. 7-11, 2003.
13) R.I. Masel (speaker), J. Ganley, E. Seebauer, I. Lee, *Microreactors for fuel conversion*, 40th Power Sources Conference, June 2002
14) S. Raimondeau (speaker), D.G. Vlachos, R.I. Masel, *Modeling of High Temperature Microchemical Systems*, 40th Power Sources Conference, June 2002
15) M.A. Shannon (speaker), G.V. Moore, J. Ganley, C. Miesse, C. Rice, E. Seebauer, R.I. Masel, *High Temperature Microcombustion Based Ammonia Microchemical Generator for PEM Fuel Cells*, 2002 Hilton Head MEMS Conference.
16) S. Raimondeau (speaker) and D.G. Vlachos, *Modeling of high temperature microreactors*, AIChE meeting, Reno NV, Nov. 4-9, 2001 Catalysis and Reaction Engineering Student Award
17) P.J.A. Kenis (speaker), J. Ganley, R.I. Masel, and M. Mitchell, *Catalytic Microreactors*, AIChE meeting, Reno NV, Nov. 4-9, 2001
18) J. Ganley (speaker), R.I. Masel, E. Seebauer, *Monolithic microreactors for the production of ammonia*, AIChE national meeting, Nov 2002
19) C. Miesse, (speaker), R.I. Masel, M.A. Shannon, *Principles of Microcombustion*, AIChE national meeting, Nov 2002
20) M. Mitchell (speaker), Christian, D.A. Dempsey, B.E. Feller, R.T. Muren, M. Wang, P.J.A. Kenis, *Microreactor for High Temperature Applications*, AIChE national meeting, Nov 2002
21) D. G. Norton, S. Raimondeau, and D. G. Vlachos, "Design rules for exothermic microchemical systems", AIChE meeting, Indianapolis, IN, Nov. 3-8, 2002, Catalysis and Reaction Engineering Student Award
22) "High Temperature Microcombustion-Based Ammonia Microchemical Hydrogen Generator Reactors for PEM Fuel Cells", with Mark Shannon, Gabriel Moore, Jason Ganley, Craig Miesse, Cynthia Rice and Edmund Seebauer, Solid-State Sensors and Actuators Workshop, Hilton Head Island, SC, June 2002 (37% acceptance rate).
23) S. Raimondeau, D. G. Vlachos, and R. I. Masel, "Modeling of high temperature microreactors," Twenty Nine *Symposium (International) on Combustion*, Sapporo, Japan, July, 2002.
24) D. G. Norton and D. G. Vlachos, "Oscillations in Microburners: Premixed methane/air mixtures" Proceedings of the Third Joint Meeting of the U.S. Sections of The Combustion

Institute, Chicago, March, 2003.
25) Hammonds Jr., J.S., and M. A. Shannon, "Modeling laser-assisted chemical etching of BSG for micromachining of MEMS structures," Proceedings of the NSF Workshop on Thermal Aspects of Material Removal Processes, June 13-18, 2003, Oklahoma.
26) Hammonds, J. S. and M. A. Shannon, "Theory of Heat Transfer for Microspaces in Chemically Reacting Systems," US-Japan Nanotherm Seminar: Nanoscale Thermal Science and Engineering, Berkeley, CA, June 24-26, 2002.
27) Shannon, M. A. "Microfabricated Mechanical Systems: Exploiting the Micro- to Nanoscale to Enhance Applications in Actuation, Sensing, and Power," Department of Mechanical and Industrial Engineering Seminar Series, University of Minnesota, Minneapolis MN, March 26, 2003.
28) Shannon, M., "Strongly Coupled Electromagnetic Fields Affect on Transport Phenomenon at the Micro- to Nanoscale," US-Japan Nanotherm Seminar: Nanoscale Thermal Science and Engineering, Berkeley, CA, June 24-26, 2002.
29) Craig Miesse, Mark Shannon, Mark Short, Rich Masel Flame Balls and Instabilities in Microcombustion, AICHE Meeting San Francisco, Nov 2003
30) J. Ganley, E. Seebauer, Rich Masel, Comparison of Catalysts For Ammonia Decomposition, AICHE Meeting San Francisco, Nov 2003
31) J. Ganley, E. Seebauer, Rich Masel, Catalytic Decomposition of Ammonia Over an Activated Porous Anodic Alumina Microreactor, AICHE Meeting San Francisco, Nov 2003
32) J. Ganley, E. Seebauer, Rich Masel, Bridging the Gap to the Hydrogen Economy: Catalytic Reforming of Fixed-hydrogen Fuels, AICHE Meeting San Francisco, Nov 2003
33) Craig Miesse, Microcombustion: Fundamental Analysis of Flame Stability and Structure, AICHE Meeting San Francisco, Nov 2003
34) Christian, M. Mitchell, I. Sung, D. A. Dempsey, D. -P. Kim, P. J. A. Kenis, “Fabrication and Characterization of Microreactors for High Temperature Applications”, AIChE Meeting, San Francisco, CA, Nov. 2003.
35) I.-K. Sung, H. Wang, X. Li, M. Mitchell, P.J.A. Kenis, D.-P. Kim (speaker) “Fabrication of Porous SiC-Based Ceramics within Microchannel Networks for High-Temperature Microreactors”, MRS Spring Meeting San Francisco Ca, April 2003.
36) R. I. Masel, "Design Rules for High Temperature Microchemical Systems," Fuel Cells for Soldier Power, Columbia, SC, Feb. 2004.
37) R. I. Masel, “Porous Microreactors For Hydrogen Production From Ammonia”, 32nd Power Sources Conference, PA, June 2004.
38) M. Short, M. Shannon, C. Miesse, R. I. Masel, “ Diffusion flame instabilities in a 0.75mm non-premixed microburner,” 30th International Symposium on Combustion, Chicago, IL, Jul. 2004.
39) R. I. Masel, “Introduction to Thermal Management for Micropower Power Sources,” Thermal Management for Micro and Meso Power Systems Conference, Chicago, IL, May 2004.
40) J. Ganley, R. I. Masel and E. G. Seebauer, “Integrated catalytic NH3 microburner/microreformer for the Production of hydrogen,” AIChE Annual Meeting, Austin, TX, Nov. 2004.
41) J. Ganley, R. I. Masel and E. G. Seebauer, “Development of a Microreactor for the Production of Hydrogen from Ammonia,” AIChE Annual Meeting, Austin, TX, Nov. 2004.
42) C. Miesse, R. I. Masel, M. Short and M. A. Shannon, “Design Rules for Microcombustors,” AIChE Annual
Meeting, Austin, TX, Nov. 2004.

43) C. Miesse, R. I. Masel, M. Short and M. A. Shannon, "Mixing in Microcombusters and Microbioreactors: Fundamentals and Applications," AIChE Annual Meeting, Austin, TX, Nov. 2004.
44) R. I. Masel, E. G. Seebauer, Zheng Ni, "The Effects of Microreactor Geometry on the Performance of Anodized Alumina Microreactor," AIChE Conference, Atlanta, GA, April 2005.
45) R. I. Masel, Zheng Ni, Vaidyanathan Subramanian, "High Surface Area Mixed Oxide Supports for High Temperature Catalysis in Micro-reactors" AIChE Conference, Atlanta, GA, April 2005
46) R. I. Masel, Craig M. Miesse, Shaurya Prakash, "Effects of Heat Transfer and Flame Stretch in Microcombustors," AIChE Conference, Altanta, GA, April 2005.
47) J. Ganley, E. G. Seebauer, R. I. Masel, "Microreactors for the Production of Hydrogen from Ammonia," AIChE Conference, Atlanta, GA, April 2005.
48) R. I. Masel, "High Temperature Microchemical Systems," DARPA Palm Power Kick-Off Meeting, Washington, D. C., Aug. 2001.
49) Energy Integration in Microchemical Devices for Hydrogen Production", AIChE meeting, Austin, TX, Nov. 7-12, 2004.
50) S. R. Deshmukh and D. G. Vlachos, "Microreactor dynamics", AIChE meeting, Austin, TX, Nov. 7-12, 2004.
51) S. Deshmukh and D. G. Vlachos, "Design Principles Of Multifunctional Microdevices", Int. Conf. Microreaction Technology (IMRET8), Spring AIChE meeting, Atlanta, GA, April 10-24, 2005.
52) S. Deshmukh and D. G. Vlachos, "Mixing In Structured Microchemical Devices", Int. Conf. Microreaction Technology (IMRET8), Spring AIChE meeting, Atlanta, GA, April 10-24, 2005.
53) S. Deshmukh, A. Mhadeshwar, and D. G. Vlachos, "Hydrogen Production from Ammonia Decomposition: Hierarchical, Multiscale Microkinetic Modeling and Microreactor Simulation", Int. Conf. Microreaction Technology (IMRET8), Spring AIChE meeting, Atlanta, GA, April 10-24, 2005.
54) P. J. A. Kenis, I. Sung, Christian, M. Mitchell (speaker), and D. P. Kim, "Fabrication and Characterization of Integrated Ceramic Microreactors for the Production of Hydrogen," AIChE National Meeting, Austin, TX, Nov. 2004.
55) P. J. A. Kenis (speaker), Christian, M. Mitchell, D. P. Kim, I. Sung, "Fabrication and Characterization of Integrated Ceramic Microreactors for High-Temperature Hydrogen Production," AICHE/IMRET national meeting, Atlanta, GA, April 2005
56) D. G. Vlachos, The emerging field of multiscale simulation in the chemical sciences, Department of Chemical and Biological Engineering, Rensselaer Polytechnic Institute, Troy, NY, Jan. 26, 2005. Invited
57) D. G. Vlachos, The emerging field of multiscale simulation in the chemical and biological sciences, Department of Chemical Engineering, UCLA, Feb. 25, 2005.
58) D. G. Vlachos, Chemical kinetics and design concepts of portable fuel processing devices, Philadelphia Catalysis Club, April 27, 2005. Invited
59) D. G. Vlachos, Design concepts of portable power generators: Hierarchical multiscale simulations and experiments, Aerospace Engineering, Univ. of Maryland, College Park, MD, May 13, 2005.
60) D. G. Vlachos, Design concepts of portable power generators: Hierarchical multiscale simulations and experiments, GE, Albany, NY, June 3, 2005. Invited
61) D. G. Vlachos, The emerging field of multiscale simulation in the chemical and biological

sciences, in Institute of Chemical Engineering and High Temperature Chemical Processes (ICE-HT), Patras, Greece, June 17, 2005. Invited
62) D. G. Vlachos, Multiscale CFD simulations of Portable Microchemical Devices for Hydrogen Production, in "Single and multiphase chemically reacting flows: CFD with detailed chemistry, population balances, fine-particle formation, and other mixing-sensitive processes" as part of the Conference on "Computational Fluid Dynamics in Chemical Reaction Engineering IV", Il Ciocco, Barga, Italy, June 26 – July 1, 2005. Invited
63) D. G. Vlachos, Combustion and partial oxidation at the microscale: Hierarchical multiscale simulations and experiments, Praxair, Buffalo, NY, Aug. 2, 2005. Invited
64) D. G. Vlachos, Design concepts for portable power generators: Hierarchical multiscale simulations and experiments, China/USA/Japan Joint Chemical Engineering Conference, Beijing, China, October 11-13, 2005. Keynote Lecture.
65) D. G. Vlachos, Hierarchical multiscale model-based design of experiments, catalysts, and reactors for portable power generators, in Emerging Applications: Microchemical and Fuel Cell Systems of the Chemical Process Control 7th (CPC7) Meeting, Lake Louise, Canada, January 8-13, 2006. Invited
66) D. G. Vlachos, The role of catalysis in the hydrogen cycle, NSF Workshop on Research Frontiers for Combustion in the Hydrogen Economy, Arlington, VA, March 9-10, 2006. Invited
67) D. G. Vlachos, Multiscale model-based process and product engineering, Imperial College, London, UK, March 17, 2006. Invited
68) D. G. Vlachos, Trends in energy research, Department of Chemical Engineering, Univ. of Patras, March 20, 2006. Invited
69) D. G. Vlachos, Catalytic Microcombustors for Compact Power Generation, Army Research Lab, Delphi, MD, April 4, 2006. Invited
70) D. G. Vlachos, The emerging field of multiscale simulation: Relation to cyber-infrastructure and educational needs, NSF Workshop on Cyber-based Combustion Science, Arlington, VA, April 19-20, 2006. Invited
71) D. G. Vlachos, Microkinetic modeling: Development, model-based design of experiments, catalysts, and reactors for fuel processing, ExxonMobil Research and Engineering Company, Annandale, NJ, June 5, 2006. Invited
72) D. G. Vlachos, Multiscale modeling of catalytic processes and catalyst synthesis, ExxonMobil Research and Engineering Company, Annandale, NJ, June 23, 2006. Invited
73) HD. G. Vlachos, ierarchical multiscale model-based design of experiments, catalysts and reactors, in 16th European Symposium on Computer Aided Process Engineering (ESCAPE) and 9th International Symposium on Process Systems Engineering (PSE), Garminsch-Partkenkirchen, Germany, July 9-13, 2006. Invited
74) D. G. Vlachos, Microkinetic modeling: Development and use, General Motors, Warren, MI, Sept. 14, 2006. Invited
75) D. G. Vlachos, Hierarchical multiscale model-based design of experiments, catalysts, and reactors for portable power generation, UPenn, Philadelphia, PA, Oct. 4, 2006. Invited
76) N. S. Kaisare and D.G. Vlachos, Extending the Region of Stable Homogeneous Micro-Combustion through Forced Unsteady Operation, Symp. Int. Comb., Heidelberg, Germany, Aug. 2006.
77) N. S. Kaisare and D.G. Vlachos, 'Stability limits of homogeneous combustion in a reverse-flow microreactor,' IMRET meeting, Postdam, Germany, Sept. 6-8, 2006.
78) Shaurya Prakash, Adrian D. Armijo, Richard I. Masel, and Mark A. Shannon, "Unsteady Flames in Microcombustion," ASME International Mechanical Engineering Congress and

Exposition November 5-10, Chicago, Illinois (accepted).

79) P.J.A. Kenis, I. Sung, Christian, M. Mitchell, D.P. Kim, SiC and SiCN materials for high temperature microreactors. Poster presented at the Thermal Management Workshop, Chicago IL, May 17-19, 2004.
80) Microscale fuel cells and fuel reformers for portable and non-portable power sources, Ohio State University, Columbus OH, June 1-2, 2005 (invited)
81) Paul J.A. Kenis, Fuel cells: Technologies, status, and why? Towards a hydrogen economy, IEEE IL Chapter, Rockford IL, September 22, 2005 (invited).
82) Paul J.A. Kenis, Fuel cells: Technologies, status, and why? Towards a hydrogen economy, UIUC Business School, November 11, 2005 (invited).
83) P.J.A. Kenis, M. Mitchell, Christian, Fabrication and characterization of integrated ceramic microreactors for hydrogen production. 231st ACS National Meeting, Atlanta GA, March 26-30, 2006.
84) P.J.A. Kenis, Christian, M. Mitchell, Development of integrated ceramic microreactors for production of hydrogen. AICHE Spring National Meeting, Orlando FL, April 23-27, 2006.
85) P.J.A. Kenis, Study of Ru/SiC monoliths for the production of hydrogen: Ammonia decomposition and propane steam reforming. AIChE National Meeting, San Francisco, CA, November 2006.
86) Paul J.A. Kenis, Microscale systems for power generation: Fuel reforming and laminar flow fuel cells, MRS Spring Meeting, San Francisco, May 2007 (invited).

5.2 Articles:

1) S. Raimondeau, D.G. Vlachos, R.I. Masel, *Modeling of High Temperature Microchemical Systems*, Proceedings 40th Power Sources Conference, 2002, 415.
2) S. Raimondeau, D. A. Norton, D. G. Vlachos, and R. I. Masel, "Modeling of high temperature microburners," *Proc. Combust. Inst.* **29**, 901-907 (2003).
3) D. G. Norton and D. G. Vlachos, "Combustion characteristics and flame stability at the microscale: A CFD study of premixed methane/air mixtures", Chem. Engng Sci. 58, 4871-4882 (2003).
4) C. Jensen, R.I. Masel, G.V Moore, M.A. Shannon, *Design rules for high temperature microburners*, Combustion Science and Technology, in Press
5) D. G. Norton and D. G. Vlachos, "A CFD study for propane/air microflame stability", Combust. Flame, **138**, 97–107 (2004).
6) S. Deshmukh, A. B. Mhadeshwar, and M. I. Lebedeva, D. G. Vlachos, "Multiscale modeling of microchemical devices: Application to hydrogen production for portable fuel cells", International Journal on Multiscale Computational Engineering **2(2)**, 221-238 (2004).
7) A. B. Mhadeshwar, J. R. Kitchin, M. A. Barteau, and D. G. Vlachos (2003) "The role of adsorbate-adsorbate interactions in the rate controlling step and most abundant reaction intermediate of NH_3 decomposition on Ru", Cat. Letters **96(1-2)**, 13-22 (2004).
8) S. R. Deshmukh and D. G. Vlachos, "CFD simulations of coupled, counter-current combustor/reformer microdevices for hydrogen production", *Ind. Eng. Chem. Res.* in press (2005).
9) S. Deshmukh, A. B. Mhadeshwar, and D. G. Vlachos "Microreactor modeling for hydrogen production from ammonia decomposition on ruthenium", Ind. Eng. Chem. Res. **43**, 2986-2999 (2004).
10) D. G. Norton and D. G. Vlachos, “Oscillations in Microburners: Premixed methane/air mixtures” Proceedings of the Third Joint Meeting of the U.S. Sections of The Combustion

Institute, Chicago, March, 2003.
11) J. Ganley, R.I. Masel, E.G. Seebauer, Porous anodic alumina posts as catalyst supports in microreactors for the production of hydrogen from ammonia, AIChE J. 50 (2004) 829-834.
12) R.I. Masel , J. Ganley, E.G. Seebauer, I. Lee, Microreactors for fuel conversion, Proceedings 40th Power Sources Conference, P367-371 (2002)
13) M.A. Shannon, G.V. Moore, J. Ganley, C. Miesse, C. Rice, E.G. Seebauer, R.I. Masel, *High Temperature Microcombustion Based Ammonia Microchemical Generator for PEM Fuel Cells*, Proceedings 2002 Hilton Head MEMS Conference.
14) A. B. Mhadeshwar, H. Wang, and D. G. Vlachos, "Thermodynamic consistency during microkinetic development of surface reaction mechanisms", J. Phys. Chem. B 107, 12721-12733 (2003).
15) Craig M Miesse, Richard I Masel, Mark Short, Mark A Shannon, "Experimental Observations of the Structure of a Diffusion Flame in a Sub-millimeter Microburner: Flame Cells and Other Unexpected Effects" Combustion Theory and Modeling, 9, 77-92, 2005.
16) Prakash, S., N. Shankar, N.G. Glumac. and M.A. Shannon, "Measurement of Hydroxyl Radical Concentration Near Surfaces with Varying Surface Activity using Laser Induced Fluorescence (LIF) Spectroscopy in Low-Pressure Stoichiometric Hydrogen/Oxygen Flames," Combustion Science and Technology, 177:4, 2005.
17) Craig M Miesse, Shaurya Prakash, Richard I Masel, Mark Short, Mark A Shannon, "Flame Cells In A Propane Diffusion Flame in a Sub-millimeter Microburner" Combustion and Flame, Submitted (2003)
18) Jason Ganley, Rich Masel, Ed Seebauer "The Effect of Catalyst Composition on the Rate of Hydrogen Production from Ammonia", Catalysis Letters, 96, 117-122, 2004.
19) Craig Miesse, Craig Jensen, Rich Masel, Mark Shannon, Mark Short, "Submillimeter Scale Combustion", AIChE Journal, 50,122 3206, 2004.
20) J. C. Ganley, R. Z. Ni, E. G. Seebauer, and R. I. Masel, "Porous Alumina Microreactors For The Production Of Hydrogen From Ammonia," Proceedings Power Sources, Proceedings Power Sources, 41, 428-431, 2004.
21) D. G. Norton, D. G., S. R. Deshmukh, E. D. Wetzel, and D. G. Vlachos, "Downsizing chemical processes for portable hydrogen production", in *Microreactor Technology and Process Intensification*, Y. Wang and J.D. Holladay, Editors. 2004, ACS: New York.
22) J. C. Ganley, K. L. Riechmann, E. G. Seebauer, R. I. Masel, "Porous Anodic Alumina Optimized as a Catalyst Support for Microreactors," J. Catalysis, 227, 26-32, 2004.
23) J. C. Ganley, E. G. Seebauer, R. I. Masel Development of a Microreactor for the Production of Hydrogen from Ammonia, J. Power Sources, 137, 1, 53-61, 2004.
24) Craig Miesse , Richard I. Masel Mark Short & Mark A. Shannon, "Diffusion flame instabilities in a 0.75mm non-premixed microburner," Proceedings of the Combustion Institute, 30, 2499-2507, 2005.
26) I.-K. Sung, Christian, M. Mitchell, D.-P. Kim, P.J.A. Kenis, "Tailored macroporous SiCN and SiC structures for high temperature fuel reforming", Advanced Functional Materials, 15, 1336-1342, 2005.
27) N. Zheng, E. G. Seebauer and R. I. Masel, "Effects of Microreactor Geometry On Performance: Differences Between Posted Reactors and Channel Reactors," Industrial and Engineering Chemistry Research, 44, 4267 4271, 2005.
28) V. Subramanian, N. Ndiege, E. G. Seebauer, M. Shannon and R. I. Masel, "Synthesis of Tantalum Pentoxide Films," Thin Solid Films, Submitted.
29) Christian, M. Mitchell, D.-P. Kim, P.J.A. Kenis, "Ceramic microreactor for on-site hydrogen

production", J. Catalysis, 241, 235-42, 2006.

30) Prakash, S., C. Miesse, R.I. Masel, and M.A. Shannon, "Flame Structure Variations in Sub-Millimeter Combustors Due to Heat Transfer through Combustor Walls," Proceedings of the Fourth Joint Meeting of the U.S. Sections of The Combustion Institute, Philadelphia, PA, March 20-23, 2005.
31) V. Subramanian, N. Ndiege, E. G. Seebauer, M. Shannon and R. I. Masel, "Synthesis of Tantalum Pentoxide Films for Waveguide Applications," Thin Solid Film, 2005, to appear.
32) R. Chandrasekharan, I. Park, R. I. Masel and M. A. Shannon, "Thermal Oxidation of Tantalum Films at Various Oxidation States From 300 to 700°C", J. Apply Phys, 98 14908, 2005.
33) R. Chandrasekharan, R. I. Masel, S. Prakash, and M. A. Shannon, "Change in Radiative Optical Properties of Tantalum Pentoxide Thin-films Due to Material Compositional Changes at High Temperature," Transaction ASME, to appear.
34) H. K. Jeong, R. Chandrasekharan, K. L. Chu, M. A. Shannon, and R. I. Masel, "Rapid Thermal Processing of Mesoporous Silica Films: A Simple Method to Fabricate Films Micrometers Thick for MEMS Applications," Industrial and Engineering Chemistry Research, 44, 8933-8937, 2005.
35) V. Subramanizn, Z. Ni, E. G. Seebauer, R. I. Masel, "Synthesis of High-Temperature Titania-Alumina Supports," Industrial & Engineering Chemistry, 45(11), 3815-3820, 2006.
36) A. D. Armijos, S. Prakash, R. I. Masel, M. A. Shannon, "Direct Imaging of Stable Methane-oxygen Flame Structures within Sub-millimeter Confined Al_2O_3 Non-premixed Combustors," Combustion Theory & Modeling, submitted.
37) S. Prakash, A. D. Armijo, R. I. Masel, M. A. Shannon, "Flame Dynamics in Sub-Millimeter Combustors," International Journal of Alternative Propulsion, 2006, to appear.
38) R. I. Masel, "Hydrogen Quick and Clean," Nature News & Views, 442, Aug. 3, 2006.
39) V. Subramanian, J. Choi, E. G. Seebauer, R. I. Masel, "TiO_2-Al_2O_3 as a Support for Propane Partial Oxidation over Rh," Catalysis Letters, submitted.
40) N. Ndiege, V. Subramanian, M. A. Shannon, and R. I. Masel, "Rapid Synthesis of Dielectric Films by Microwave Assisted CVD," Chemical Communications, submitted
41) J. Yeom, J.H. Han, B. Bae, M. A. Shannon, "Design and Characterization of Micropost-filled Reactor to Minimize Pressure Drop while Maximizing Surface-area-to-volume-ratio," *IMECE 2006*, Nov. 2006 Chicago, IL, pg.
42) D. G. Norton, S. R. Deshmukh, E. D. Wetzel, and D. G. Vlachos, Downsizing chemical processes for portable hydrogen production, in Microreactor Technology and Process Intensification, Y. Wang and J.D. Holladay, Editors. ACS: New York, Vol. 914, 179-193 (2005).
43) S. R. Deshmukh and D. G. Vlachos, "CFD simulations of coupled, counter-current combustor/reformer microdevices for hydrogen production", Ind. Eng. Chem. Res. 44, 4982-4992 (2005).
44) S. R. Deshmukh and D. G. Vlachos, "Effect of flow configuration on the operation of coupled combustor/reformer microdevices for hydrogen production", Chem. Engng Sci. 60, 5718-5728 (2005).
45) S. R. Deshmukh and D. G. Vlachos, "Novel micromixers driven by flow instabilities: Application to post-reactors", AIChE J. 51, 3193-3204 (2005).
46) N. S. Kaisare and D. G. Vlachos, "Optimal Reactor Dimensions for Homogeneous Combustion in Small Channels", Catal. Today accepted (2005).

47) N. S. Kaisare and D. G. Vlachos, "Extending the Region of Stable Homogeneous Micro-Combustion through Forced Unsteady Operation", Proc. Combust. Inst. 31, in press (2006).
48) D. G. Vlachos, A. B. Mhadeshwar, and N. Kaisare, "Hierarchical multiscale model-based design of experiments, catalysts, and reactors for fuel processing", Comput. Chem. Eng. 30, 1712-1724 (2006).
49) Chandrasekharan, R., S. Prakash, R.I. Masel, M.A. Shannon, "Change in radiative optical properties of TA_2O_5 thin-films due to high temperature Heat Treatment," *Journal of Heat Transfer,* (in press 2006).
50) Shaurya Prakash, Adrian D. Armijo, Richard I. Masel, and Mark A. Shannon, "Unsteady Flames in Microcombustion," *Proceedings of IMECE 2006* ASME International Mechanical Engineering Congress and Exposition November 5-10, Chicago, Illinois *(accepted).*
51) Shaurya Prakash, Adrian D. Armijo, Richard I. Masel, and Mark A. Shannon, "Flame Dynamics and Structure within Sub-Millimeter Combustors," *AIChE Journal (submitted 2006).*
52) Christian, M. Mitchell, and P. J. A. Kenis, "Fabrication and characterization of integrated ceramic microreactors for hydrogen production", *Proceedings of the 231st ACS National Meeting*, **,** Atlanta GA, March 26-30, 2006.
53) P.J.A. Kenis, A.D. Stroock, "Materials for micro- and nanofluidics", *MRS Bulletin*, Vol. 31, , pp. 87-90, February 2006.
54) Christian, M. Mitchell, P.J.A. Kenis, "Ceramic microreactors for on-site hydrogen production from high temperature steam reforming of propane", *Lab on a Chip*, 6, 1328-1337, 2006.
55) P.J.A. Kenis, Christian, M. Mitchell, "Production of Hydrogen for Fuel Cell-based Power Sources", *Catalysis Today (*2007*)*, invited.